→ 3rd ADVANCED COURSE ON RADAR POLARIMETRY

Polarimetric SAR Tomography Advanced concepts

PolTomSAR using spectral estimation techniques

Laurent Ferro-Famil, University of Rennes 1, France

Stefano Tebaldini, Politecnico di Milano, Italy

19–23 January 2015 | ESA-ESRIN | Frascati (Rome), Italy

European Space Agency

Synthetic Aperture Radar (SAR)

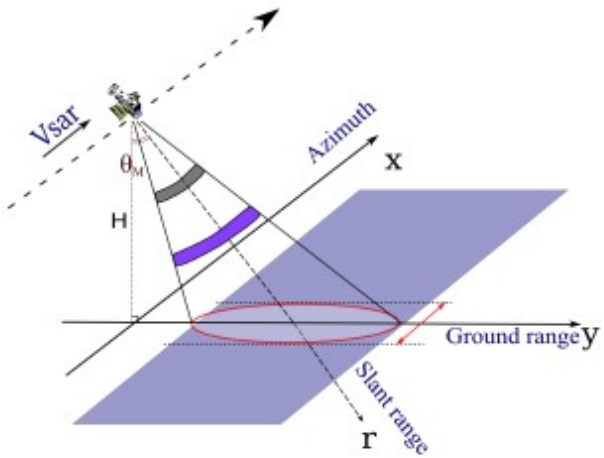

- Large-scale imaging, all-weather capabilities, high spatial resolution . . .
- Sensitive to earth surface properties, volume density, moisture . . .
- Adapted to forest biomass estimation and urban area characterization.

SAR image

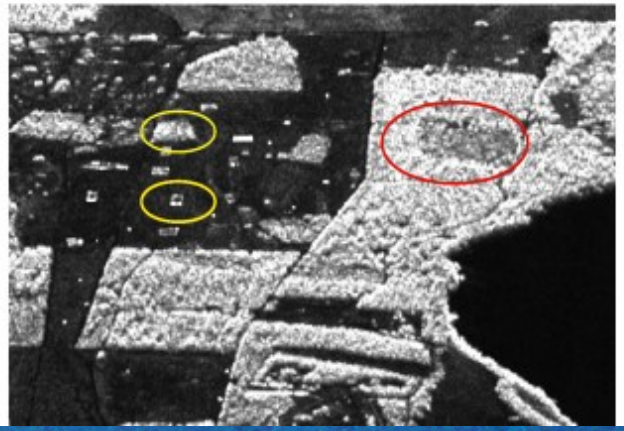

- Ambiguous identification
- No structure information.

PolSAR principles

Polarimetric SAR (PolSAR)

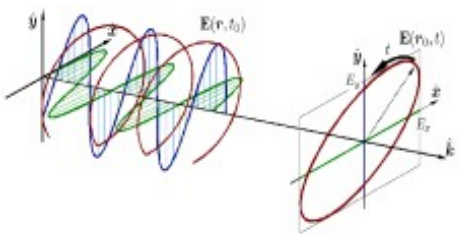

$$\mathbf{S} = \begin{bmatrix} S_{hh} & S_{vh} \\ S_{hv} & S_{vv} \end{bmatrix} \rightarrow \mathbf{k} = \frac{1}{\sqrt{2}} \begin{bmatrix} S_{hh} + S_{vv} \\ S_{hh} - S_{vv} \\ S_{hv} + S_{vh} \end{bmatrix} \rightarrow \mathbf{T} = E\{\mathbf{k}\mathbf{k}^{\dagger}\}$$

Over forested areas

|HH+VV| |HH-VV| |HV|

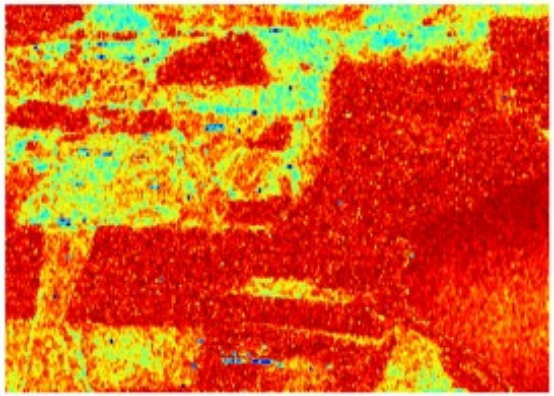

Entropy (H)

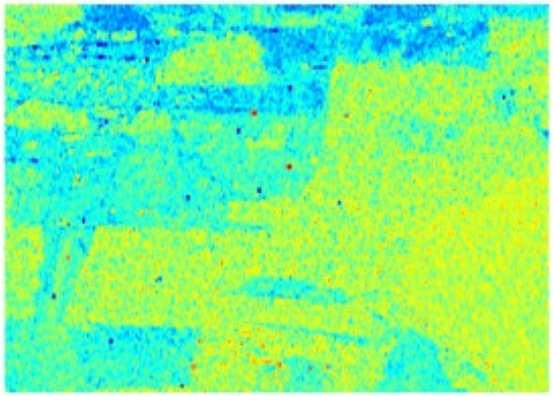

α

☺ Enhanced discrimination possibilities

☹ Saturation over dense volumes

Pol-inSAR principles

Polarimetric SAR interferometry (PolInSAR)

Polarization-dependent interferometric phase

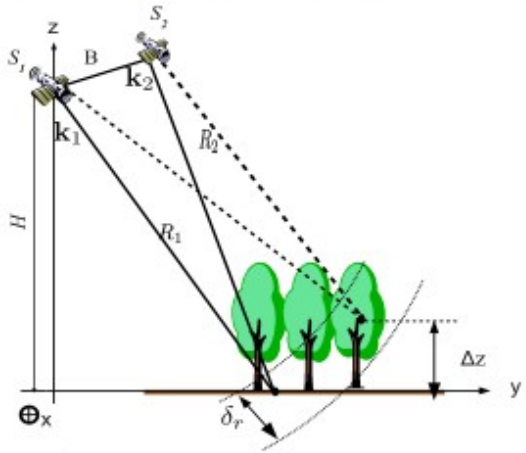

$$\mathbf{k} = \begin{bmatrix} \mathbf{k}_1 \\ \mathbf{k}_2 \end{bmatrix} \quad \mathbf{T} = \langle \mathbf{k}\mathbf{k}^\dagger \rangle = \begin{bmatrix} \mathbf{T}_3 & \mathbf{T}_{12} \\ \mathbf{T}_{12}^\dagger & \mathbf{T}_3 \end{bmatrix}$$

$$\gamma(\boldsymbol{\omega}) = \frac{\boldsymbol{\omega}^\dagger \mathbf{T}_{12} \boldsymbol{\omega}}{\boldsymbol{\omega}^\dagger \mathbf{T}_3 \boldsymbol{\omega}} \Rightarrow \phi_{topo}(\boldsymbol{\omega}) = k_z \Delta z(\boldsymbol{\omega})$$

Discrimination of phase centres according to polarisation

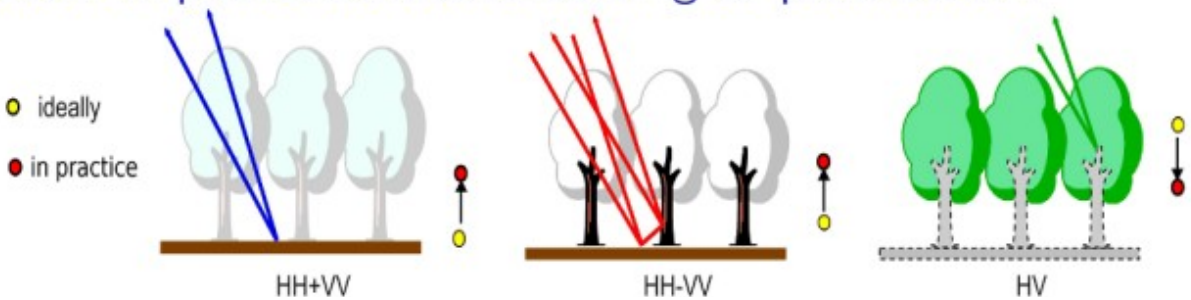

Cloude, S. & Papathanassiou, K. "Polarimetric SAR interferometry" IEEE TGRS, 1998
Papathanassiou, K. & Cloude, S, "Single-baseline polarimetric SAR interferometry," IEEE TGRS 2001
Cloude, S. & Papathanassiou, K. "Three-stage inversion process for polarimetric SAR interferometry", IEE RSN, 2003

SAR Tomography principles

Multibaseline InSAR (MB-InSAR) tomography

Acquisition geometry

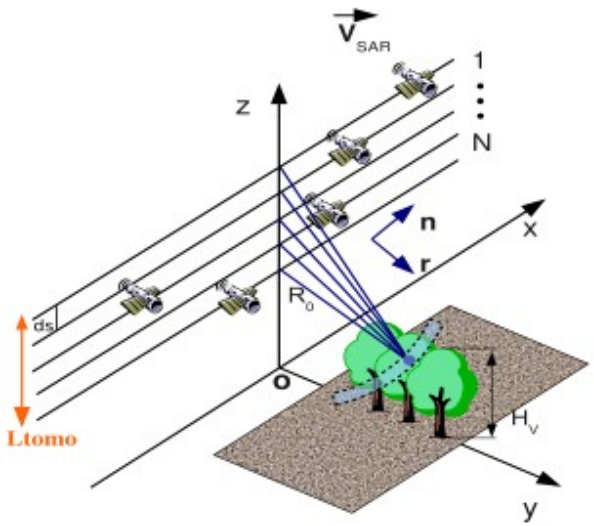

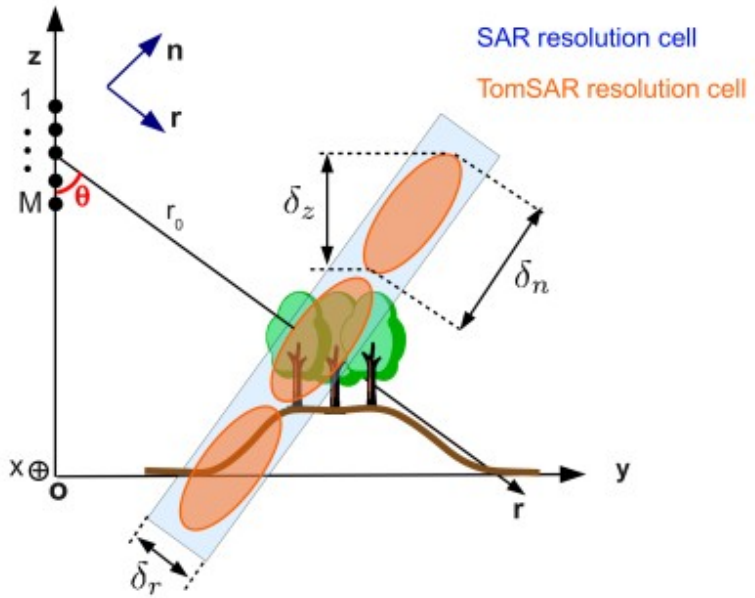

Vertical focusing

- Vertical aperture : L_{tomo}
- Resolution : $\delta_z = \delta_n \sin\theta$ with $\delta_n = \frac{\lambda R_0}{2L_{tomo}}$

Reigber, A. & Moreira, A. "First demonstration of airborne SAR tomography using multibaseline L-band data", IEEE TGRS, 2000

Polarimetric SAR Tomography principles

Multibaseline polarimetric SAR tomography

MB SAR Tomography

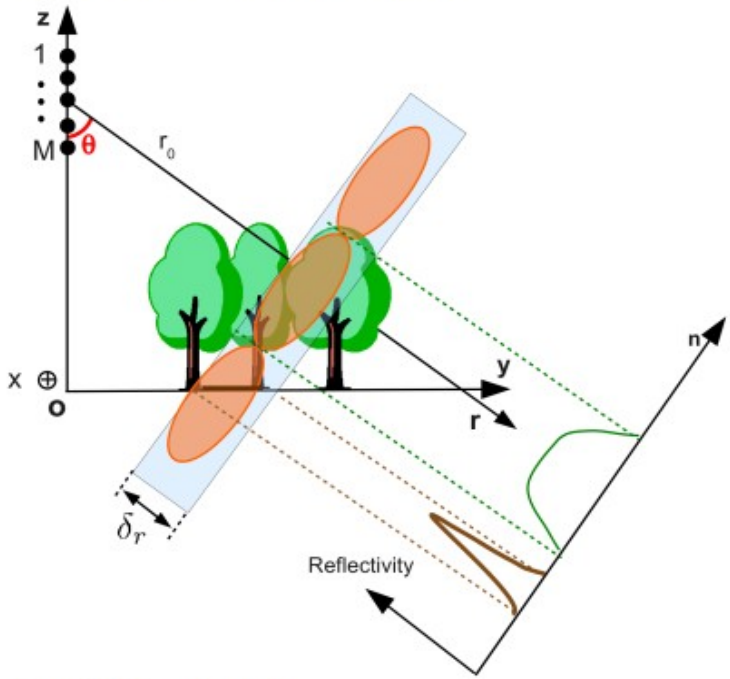

TomoSAR : reflectivity

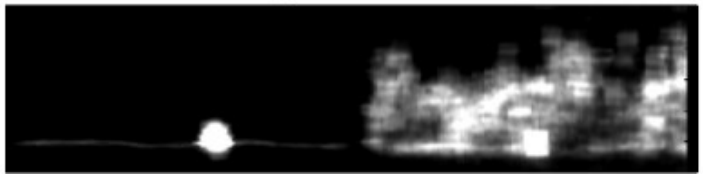

Polarimetric MB SAR Tomography

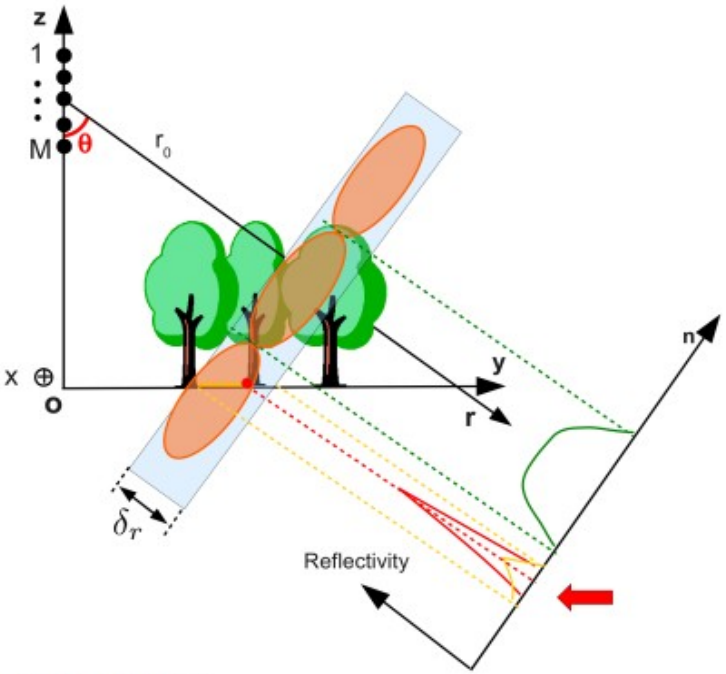

PolTomSAR: α

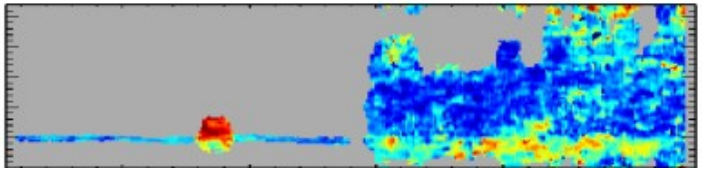

Tebaldini, S. "Algebraic Synthesis of Forest Scenarios From Multibaseline PolInSAR Data", IEEE TGRS 2009
Tebaldini, S. "Single and Multipolarimetric SAR Tomography of Forested Areas: A Parametric Approach" IEEE TGRS 2010
L. Ferro-Famil, Y. Huang, E. Pottier, "Principles and applications of polarimetric SAR tomography for the characterization of complex environments", IAGS proceedings, 2014

Polarimetric SAR Tomography principles

MB-InSAR data model (M acquisitions)

Single-pol case

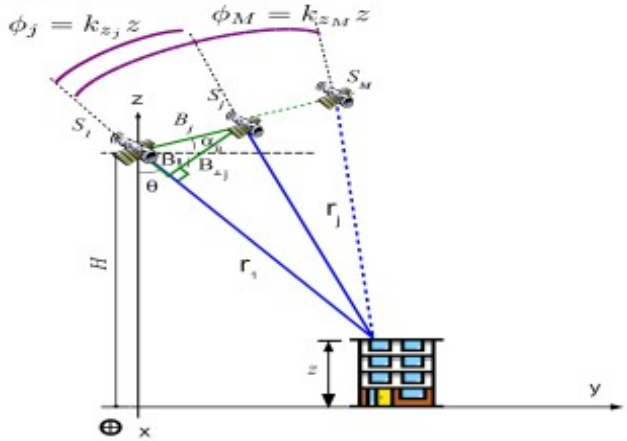

- $\mathbf{y} = [y_1, \ldots, y_M]^T$
- $\mathbf{a}(z) = [1, e^{jk_{z_2} z}, \ldots, e^{jk_{z_M} z}]^T$
- Sum of D contributions
  $\mathbf{y}(l) = \sum_{i=1}^{D} \sqrt{\sigma_i} \mathbf{x}_i(l) \odot \mathbf{a}(z_i) + \mathbf{n}(l)$

Full pol case

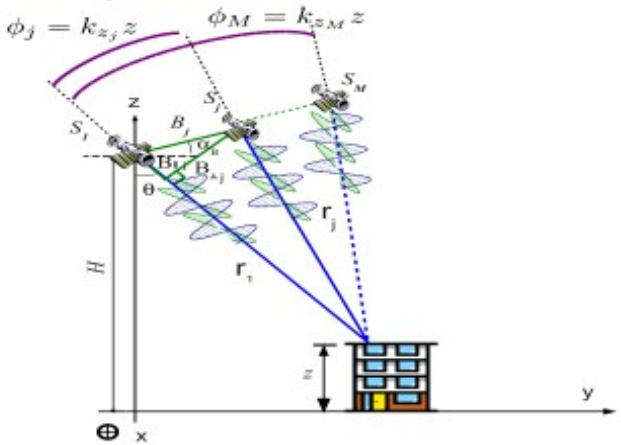

- $\mathbf{y} \rightarrow \mathbf{y}_P = \begin{bmatrix} \mathbf{y}_1 \\ \mathbf{y}_2 \\ \mathbf{y}_3 \end{bmatrix}$, $\mathbf{a}(z) \rightarrow \mathbf{a}(z, \mathbf{k}) = \mathbf{k} \otimes \mathbf{a}(z)$
- Polarimetric target vector $\mathbf{k} = [k_1, k_2, k_3]^T$

MB-InSAR signal models

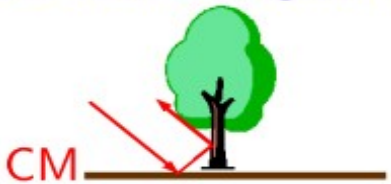

CM

$\mathbf{x}_{c_i} = \mathbf{1}_{(M \times 1)}$

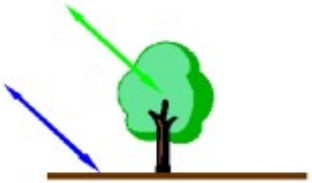

UM

$\mathbf{x}_{u_i} \sim \mathcal{N}(0, \mathbf{R}_{ii})$

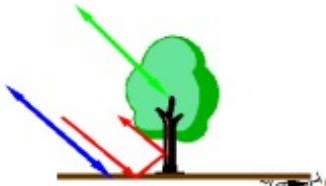

HM

Objectives of PolTomSAR focusing

Discrete case (N_s sources)

- Heights : $\hat{\mathbf{z}}$
- Reflectivities : $\hat{\boldsymbol{\sigma}}$
- Pol. info. : $\hat{\mathbf{K}}$

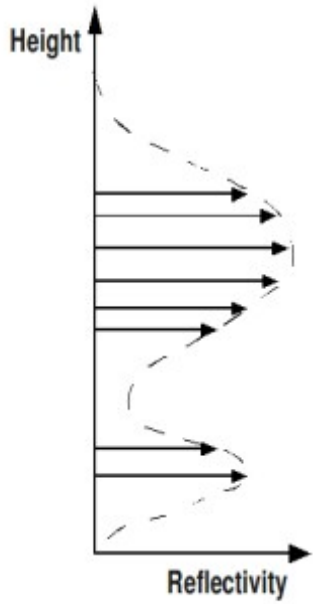

Continuous case

- Reflectivity : $\hat{\sigma}(z)$
- Pol. info. :
  - $\mathbf{k}(z)$
  - $\mathbf{T}(z) = \mathrm{E}(\mathbf{k}(z)\mathbf{k}^{\dagger}(z))$

Practical implementation

- Parameters estimated from $\hat{\mathbf{R}} = \frac{1}{L}\sum_{l=1}^{L}\mathbf{y}(l)\mathbf{y}(l)^{\dagger}$
- N_s : estimated using MOS techniques
- Various types of estimators :
  - Beamformer, Capon, Music
  - ML, Subspace Fitting

Polarimetric SAR Tomography principles

Acquired CM signal (single scatterer)

$$\mathbf{y} = a_c\,\mathbf{a}(z_0) + \mathbf{n}$$

with $\mathbf{a}(z_0) = [1, \mathrm{e}^{jk_{z_2} z_0}, \ldots, \mathrm{e}^{jk_{z_M} z_0}]^T$

Proposed approach: linear filtering

$$f(\mathbf{w}) = \mathbf{w}^\dagger \mathbf{y} = \sum_{i=1}^{M} w_i^* y_i$$

Objective

$$p(\mathbf{w}_{opt}) = |f(\mathbf{w}_{opt})|^2 = |\hat{a}_c|^2$$

Beamformer

- adapted filter maximizing the output SNR: $\mathbf{w}_{BF} = \dfrac{\mathbf{a}(z)}{M}$
- SNR maximized at z = z_0 : $\hat{z}_0 = \arg\max_z |f(z)|^2$
- Reflectivity estimate: $|f(\hat{z}_0)|^2 \approx |a_c|^2$

Polarimetric SAR Tomography principles

Uniform baseline sampling $\mathbf{a}(z) = [1, \mathrm{e}^{j\mathrm{d}k_z z}, \ldots, \mathrm{e}^{j(M-1)\mathrm{d}k_z z}]^T$

$$|f(z)| = |a_c| \frac{\mathbf{a}^\dagger(z)\mathbf{a}(z_0)}{N} = \frac{|a_c|}{M} \frac{|\sin(\pi \Delta k_z (z - z_0))|}{|\sin(\pi \mathrm{d} k_z (z - z_0))|}$$

Spatial features of a tomogram

- **rapidly varying: resolution**
- **band-limited: sidelobes**
- **sampled: ambiguities**

$$\delta z = \frac{2\pi}{\Delta k}, \quad z_{amb} = \frac{2\pi}{\mathrm{d}k}, \quad \delta z = \frac{z_{amb}}{M}$$

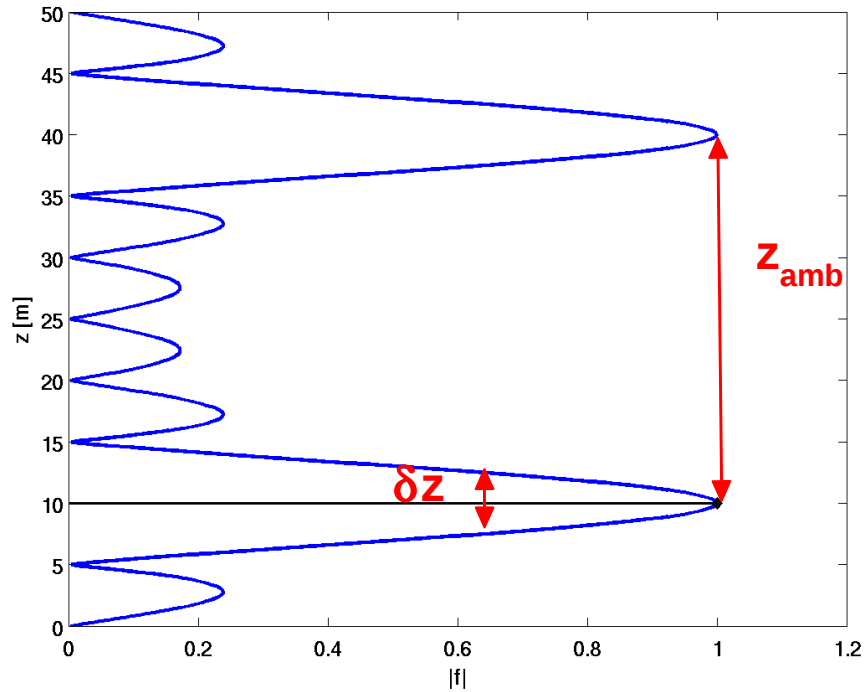

M=6

Polarimetric SAR Tomography principles

M=6

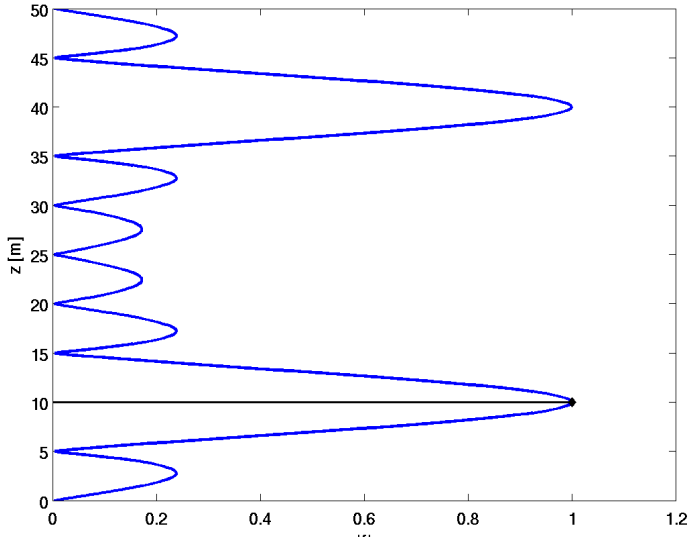

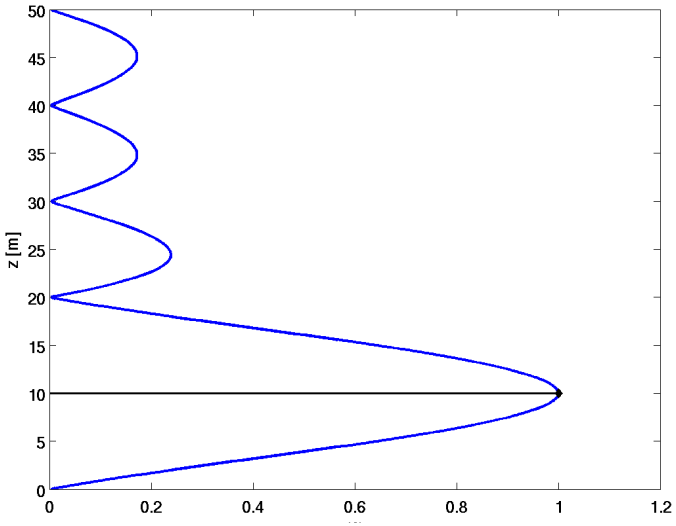

M=12

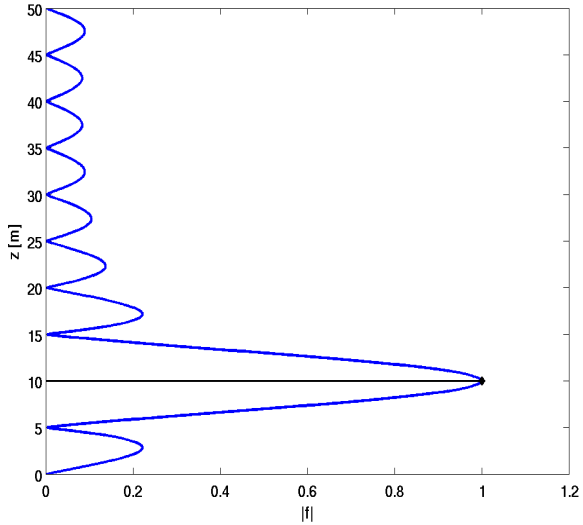

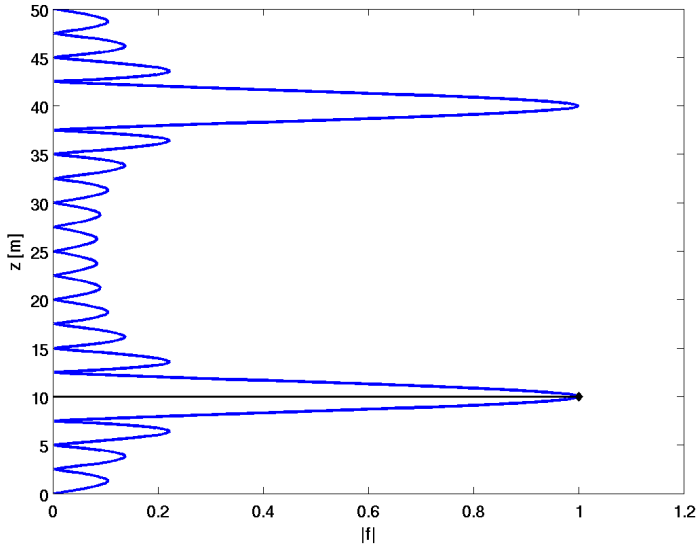

Polarimetric SAR Tomography principles

Beamformer features

- Excellent statistical accuracy
- Poor resolution
- Cannot handle closely spaced scatterers

Capon's approach

- Linear filter
- Aims to minimize spatial perturbations & sidelobes

$$\mathbf{w}_C = \arg\min_{\mathbf{w}} \mathrm{E}(\mathbf{w}^\dagger \mathbf{y}) \quad \text{s.t.} \quad \mathbf{w}^\dagger \mathbf{a}(z) = 1$$

$$\mathbf{w}_C = \frac{\mathbf{R}^{-1}\mathbf{a}(z)}{\mathbf{a}^\dagger(z)\,\mathbf{R}^{-1}\mathbf{a}(z)}, \quad \mathbf{R} = \mathrm{E}(\mathbf{y}\mathbf{y}^\dagger)$$

For UM (stochastic) signals

Speckle filtering $P(z) = E(|\hat{a}_c|^2) = E(|\mathbf{w}^\dagger \mathbf{y}|^2) = \mathbf{w}^\dagger \mathbf{R} \mathbf{w}$

Multilook estimates $P_{BF}(z) = \mathbf{a}^\dagger(z)\mathbf{R}\mathbf{a}(z), \quad P_C(z) = \dfrac{1}{\mathbf{a}^\dagger(z)\mathbf{R}^{-1}\mathbf{a}(z)}$

In practice $\widehat{\mathbf{R}} = \dfrac{1}{L}\sum_{l=1}^{L} \mathbf{y}(l)\mathbf{y}^\dagger(l)$

Polarimetric SAR Tomography principles

Tropical forest profile at P band

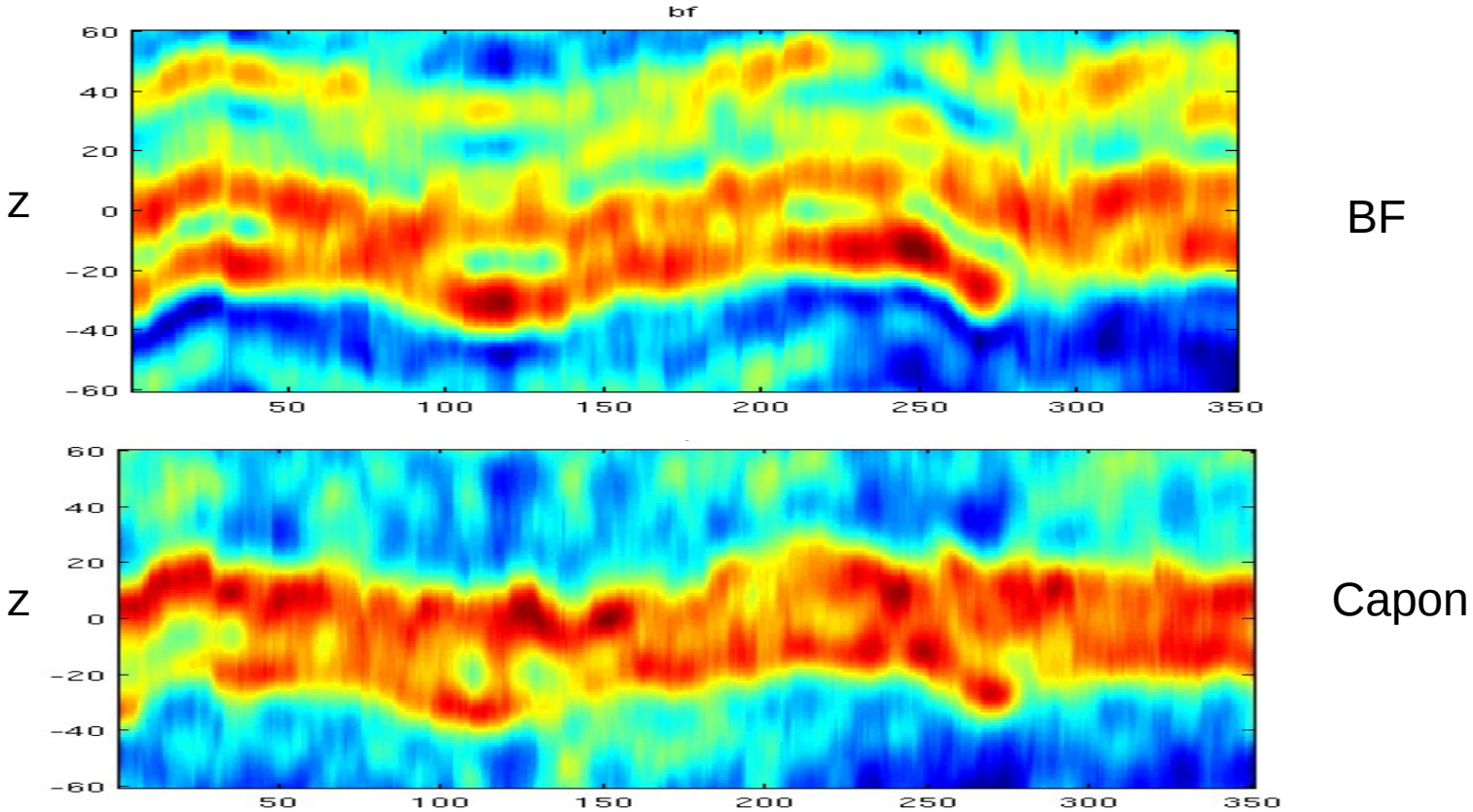

Polarimetric SAR Tomography principles

Critical configuration (**3 images**) in an urban environment at L band

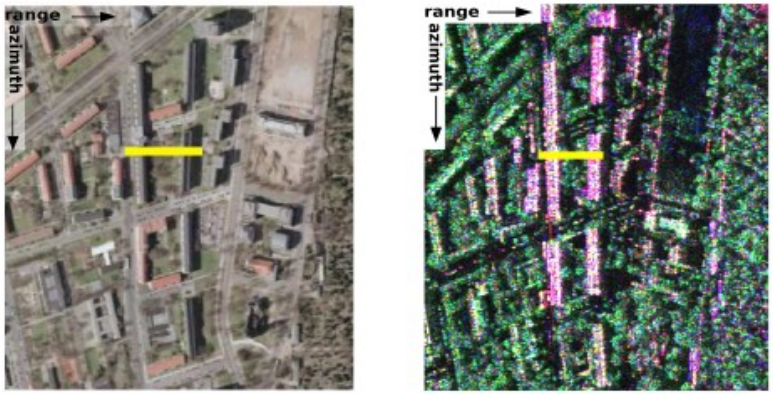

(a) Optical image (b) SAR

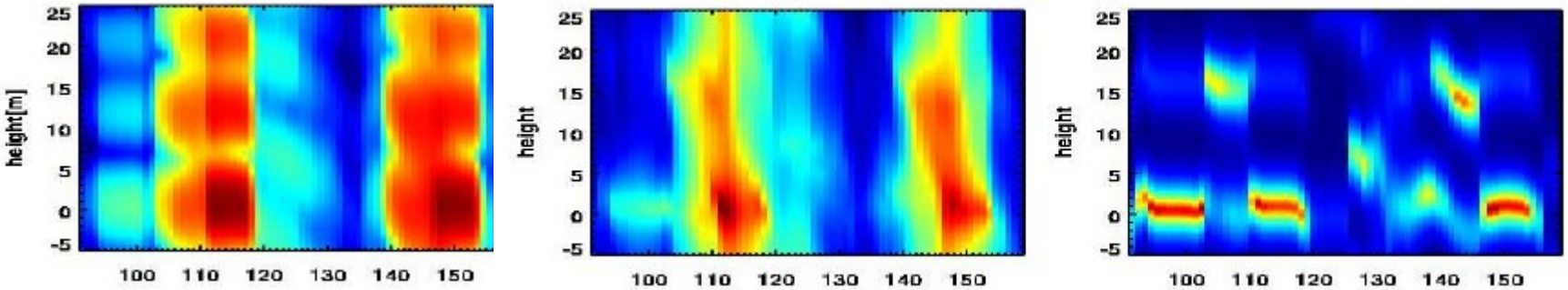

BF CAPON MUSIC

Strictly speaking, Capon's technique is not HR, but is very convenient and can be easily derived in the full-pol case

Classical (rank 1) FP Beamforming and Capon

MB-POLinSAR signals

- Scatterer characteristics :

$$\text{Elevation } z_i \rightarrow \mathbf{a}(z_i) \text{ \& target vector } \mathbf{v_i} = s_i \mathbf{k_i} \in \mathbb{C}^{3\times 1}$$

- Separate processing of $\mathbf{y}_{pp}$, $\mathbf{y}_{pq}$, $\mathbf{y}_{qq}$:
  - Different elevation estimates : $\hat{z}_{pp}$, $\hat{z}_{pq}$, $\hat{z}_{qq}$
  - Incoherent estimates : relative phase information is missing
  - Estimates depend on the chosen basis
- Joint polarimetric processing :

$$\mathbf{y}_P = \begin{bmatrix} \mathbf{y}_1 \\ \mathbf{y}_2 \\ \mathbf{y}_3 \end{bmatrix} \in \mathbb{C}^{3M\times 1} \quad \Rightarrow \mathbf{y}_{P_i} = s_i \begin{bmatrix} k_{1_i}\mathbf{a}(z_i) \\ k_{2_i}\mathbf{a}(z_i) \\ k_{3_i}\mathbf{a}(z_i) \end{bmatrix} + \mathbf{n} = s_i \mathbf{a}(z_i, \mathbf{k}_i) + \mathbf{n}$$

- Polarimetric steering vector : $\mathbf{a}(z_i, \mathbf{k}_i) = k_i \otimes \mathbf{a}(z_i)$

Parameters to estimate from second order statistics $\mathbf{R}_P = \mathrm{E}(\mathbf{y}_P \mathbf{y}_P^\dagger)$

- Elevation z_i, reflectivity $\sigma_i = \mathrm{span}_i = \mathrm{E}(|s_i|^2)$,unitary target vectors $\mathbf{k}_i$
- Over continuous media :$\sigma(z), \mathbf{k}(z)$

Classical (rank 1) FP Beamforming and Capon

Objective functions

- $P_B(z,\mathbf{k}) = \frac{\mathbf{a}^\dagger(z,\mathbf{k})\hat{\mathbf{R}}_P\mathbf{a}(z,\mathbf{k})}{M^2}$, $P_C(z,\mathbf{k}) = \frac{1}{\mathbf{a}^\dagger(z,\mathbf{k})\hat{\mathbf{R}}_P^{-1}\mathbf{a}(z,\mathbf{k})}$
- Reformulation : $\mathbf{a}(z,\mathbf{k}) = \mathbf{B_a}(z)\mathbf{k}$

$$P_B(z,\mathbf{k}) = \frac{\mathbf{k}^\dagger\mathbf{M}_B(z)\mathbf{k}}{M^2},\ P_C(z,\mathbf{k}) = \frac{1}{\mathbf{k}^\dagger\mathbf{M}_C(z)\mathbf{k}}$$

- "Focused" matrices :

$$\mathbf{M}_B(z) = \mathbf{B}_\mathbf{a}^\dagger(z)\hat{\mathbf{R}}_P\mathbf{B_a}(z) > \mathbf{0},\ \mathbf{M}_C(z) = \mathbf{B}_\mathbf{a}^\dagger(z)\hat{\mathbf{R}}_P^{-1}\mathbf{B_a}(z) > \mathbf{0}$$

Parameter estimation : eigen-problem

$$P_B(z) = \max_\mathbf{k} P_B(z,\mathbf{k}) = \frac{\lambda_{max}(\mathbf{M}_B(z))}{M^2},\ P_C(z) = \max_\mathbf{k} P_C(z,\mathbf{k}) = \frac{1}{\lambda_{min}(\mathbf{M}_C(z))}$$

- Span : $\sigma_i = P_{B,C}(z_i)$
- Dominant scattering vector : $\hat{\mathbf{k}}_{B_i} = \mathbf{e}_{max}(\mathbf{M}_B(z))$, $\hat{\mathbf{k}}_{C_i} = \mathbf{e}_{min}(\mathbf{M}_C(z))$

Full rank FP Beamforming and Capon

Source characteristics

- Elevation z_i, polarimetric covariance matrix $\mathbf{T} = \mathrm{E}(\mathbf{v}\mathbf{v}^\dagger) \in \mathbb{C}^{3\times 3}$
- Eigen-decomposition $\mathbf{T} = \mathbf{U}\mathbf{\Lambda}\mathbf{U}^\dagger = \sum_{j=1}^{3} \lambda_j \mathbf{u}_j \mathbf{u}_j^\dagger$ with $\mathbf{u}_i^\dagger \mathbf{u}_j = \delta_{i-j}$

Beamformer full rank FP estimator

$$\hat{\mathbf{T}}_B(z) = \frac{1}{M^2}\mathbf{M}_B(z)$$

Capon full rank FP estimator

$$\hat{\mathbf{T}}_C(z) = \mathbf{M}_C^{-1}(z)$$

3-D (x,y,z) coherency matrices can be generated and processed like usual 2-D images, i.e. with PolSARpro!

3-D IMAGING OF AN URBAN AREA USING A MINIMAL POL-TOMSAR CONFIGURATION

Urban area test site

- Images over Dresden, 2000
- DLR's E-SAR at L-Band
- Resolution : 0.5 m × 2.5 m
- Fully polarimetric
- Dual-baseline InSAR

Baselines	H_{am}
10 m	55-73 m
40 m	14-18 m

3 PolSAR images

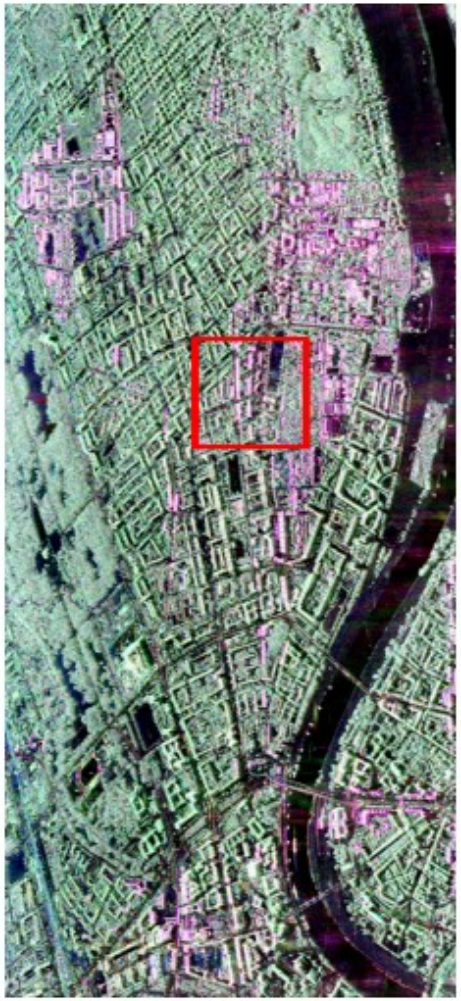

Pauli-coded SAR image

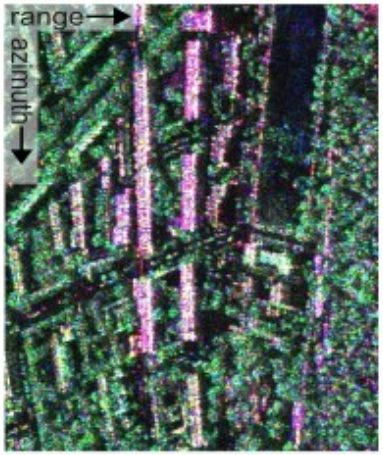

Optical image

L. Ferro-Famil, Y. Huang, E. Pottier, "Principles and applications of polarimetric SAR tomography for the characterization of complex environments", IAGS proceedings, 2014

Polarimetric SAR tomography over urban areas

Performance evaluation results

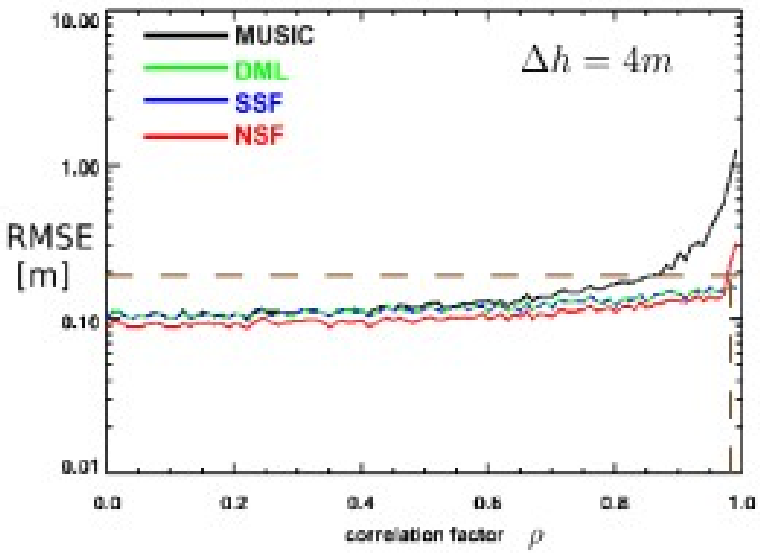

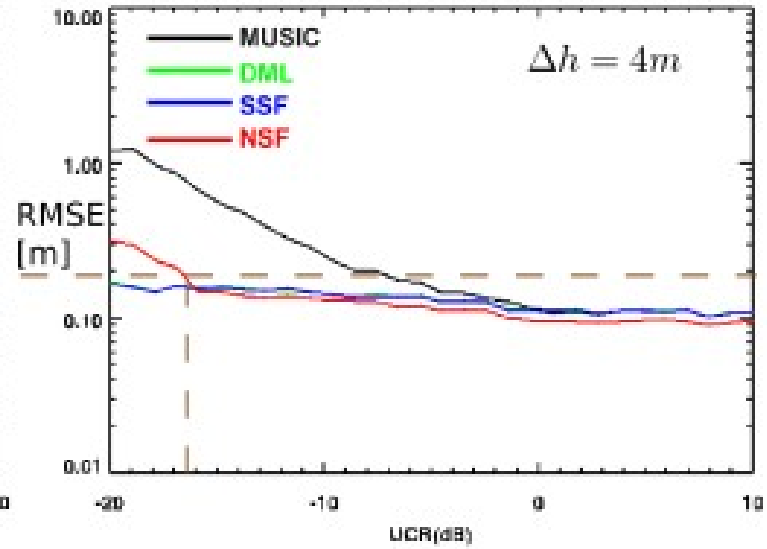

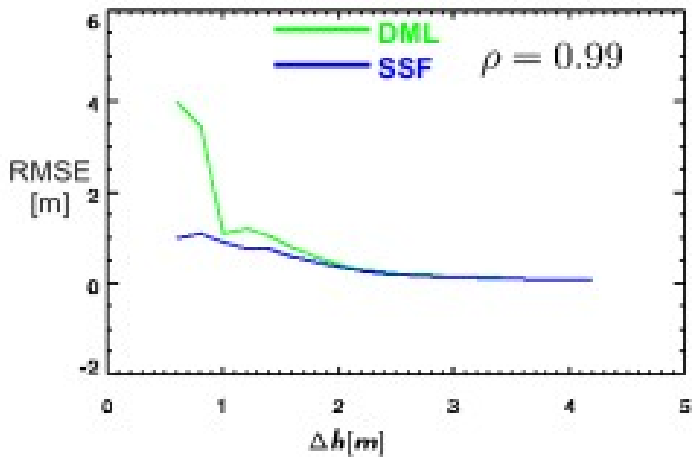

- $\rho = 0.98$ equivalent to $UCR = -16dB$
- SSF: adaptive to scatterers
- NSF: optimal resolution if $\rho \neq 1$

Polarimetric SAR tomography over urban areas

- Scattering mechanisms: $\mathbf{k_1}$, $\mathbf{k_2}$ with polarization difference $\zeta = acos(\frac{\mathbf{k_1}^{\dagger}\mathbf{k_2}}{\sqrt{|\mathbf{k_1}|^2|\mathbf{k_2}|^2}})$

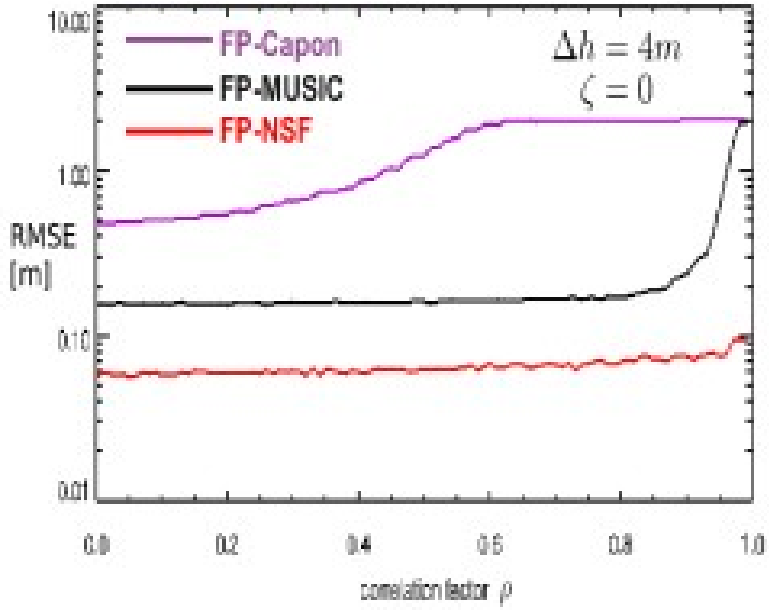

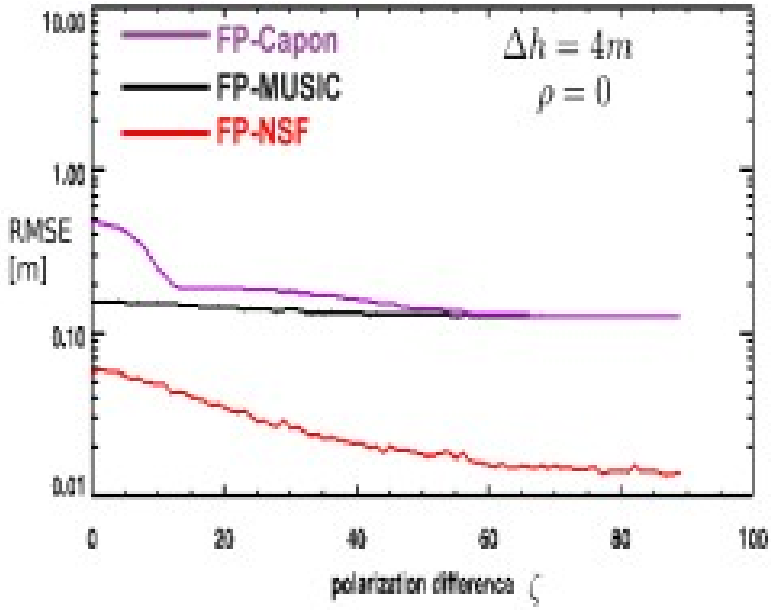

- FP-NSF: better than SP case for higly correlated scatterers
- FP-Capon: similar to FP-MUSIC when $\zeta \geq 60°$

Polarimetric SAR tomography over urban areas

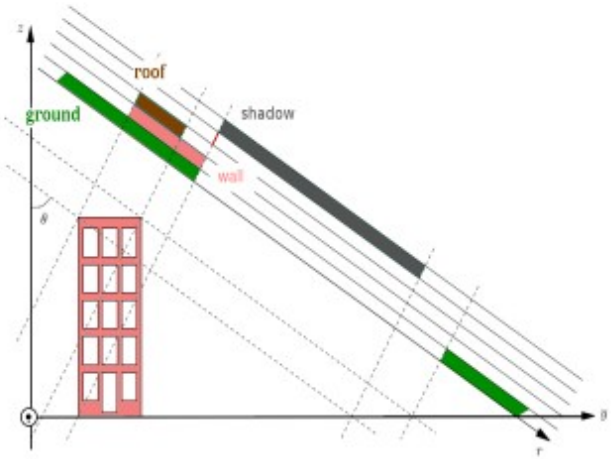

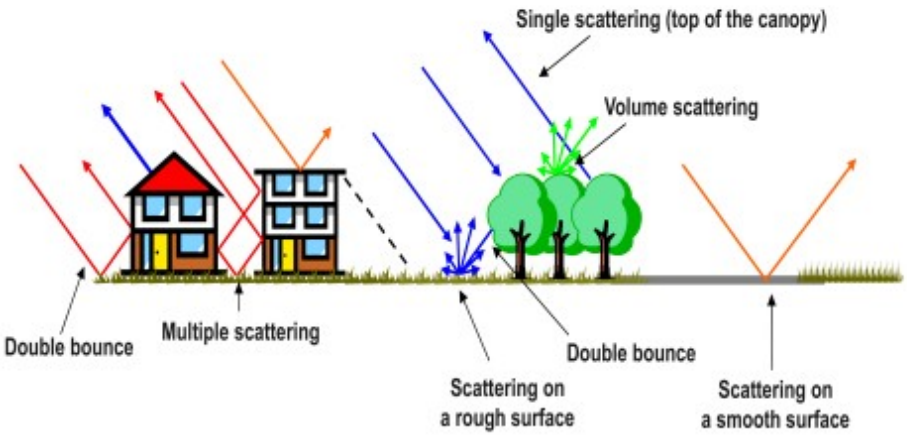

- L-band intermediate-resolution data sets
  $\Rightarrow$ High-Resolution (HR) tomographic estimators
- 3 images
  $\Rightarrow N_s = 2$
- Sum of diverse (polarimetric & statistical) contributions
  $\Rightarrow$ FP-NSF model adaptive estimator.

Polarimetric SAR tomography over urban areas

Surface elevation map

LiDAR

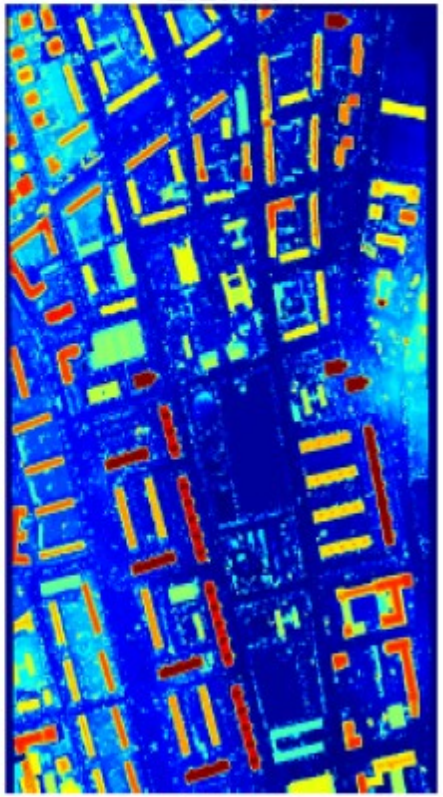

Estimated by FP-NSF ($N_s = 2$)

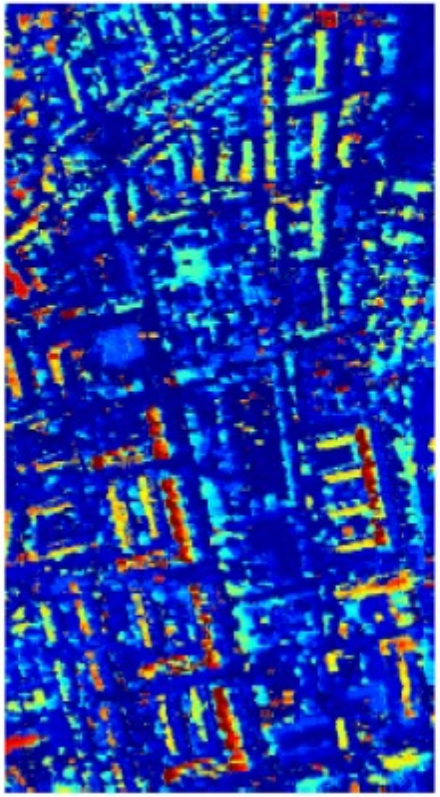

Polarimetric SAR tomography over urban areas

Building reconstruction

Google map

Pauli-coded

LiDAR

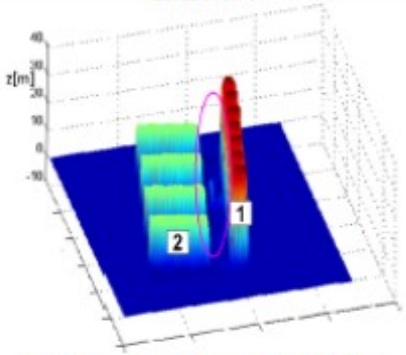

Estimated by FP-NSF
($N_s = 2$)

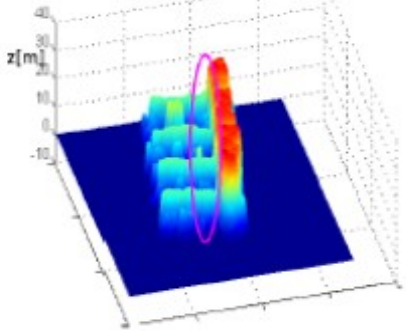

Difference between LiDAR and estimated surface

- projection of SAR imaging
- vegetation between B1 and B2

Polarimetric SAR tomography over urban areas

Building reconstruction

Google map

Bing map

LiDAR

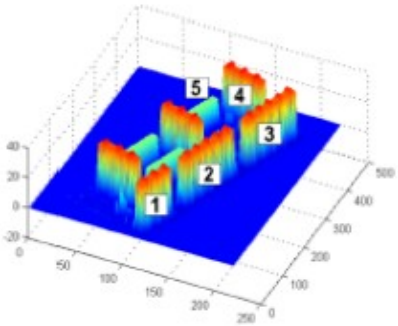

Estimated by FP-NSF
($N_s = 2$)

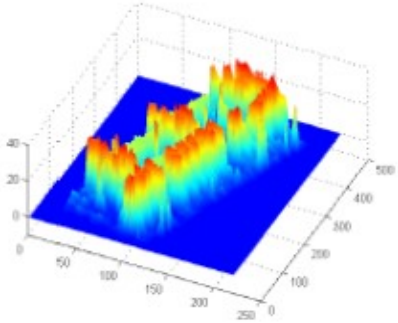

Averaged z[m]	B1	B2	B3	B4	B5
LIDAR	30.0	30.2	30.1	30.8	16.3
Estimated	27.5	27.8	27.5	27.3	16.1

POL-TOMSAR IMAGING OF CONCEALED OBJECTS

Above ground and under foliage objects observed at L band

- DLR E-SAR image over Dornstetten, Germany
- L-Band
- 21 tracks : average baseline 20m
- $\delta_z = 2$m

Horizontal baseline distribution

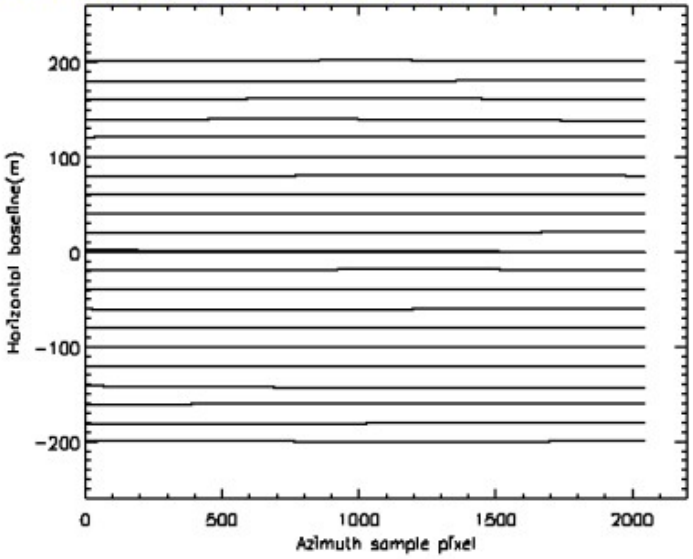

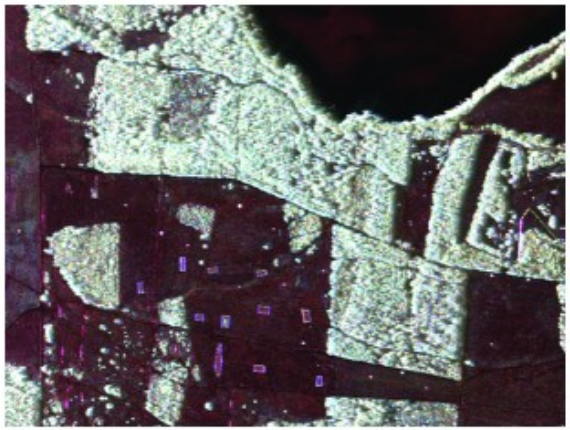

Huang, Y.; Ferro-Famil, L. & Reigber, A. "Under-Foliage Object Imaging Using SAR Tomography and Polarimetric Spectral Estimators", IEEE TGRS 2011

VV refectivity tomograms

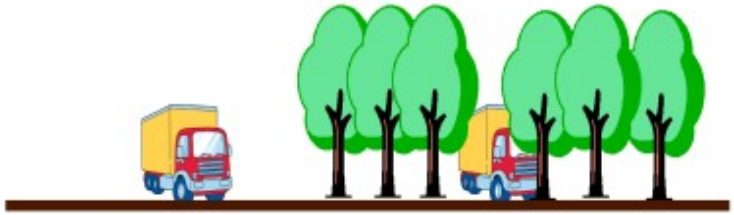

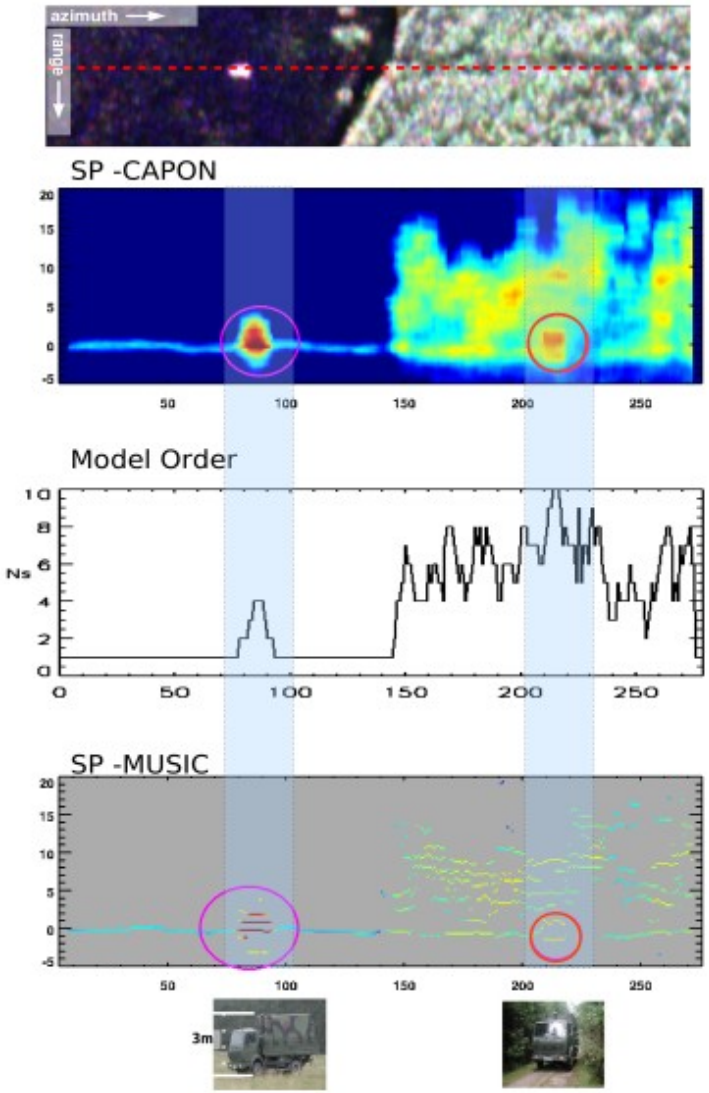

Capon :

limited resolution
$\Rightarrow$ overestimated H_{truck}

MUSIC :

- ☺ Sub-canopy truck
  $\Rightarrow$ hybrid scatterer
- ☹ Uncovered
  $\Rightarrow$ coherent scatterer
- ☹ Spurious sidelobes.

High Resolution tomograms of underfoliage objects

SSF : shape and reflectivity

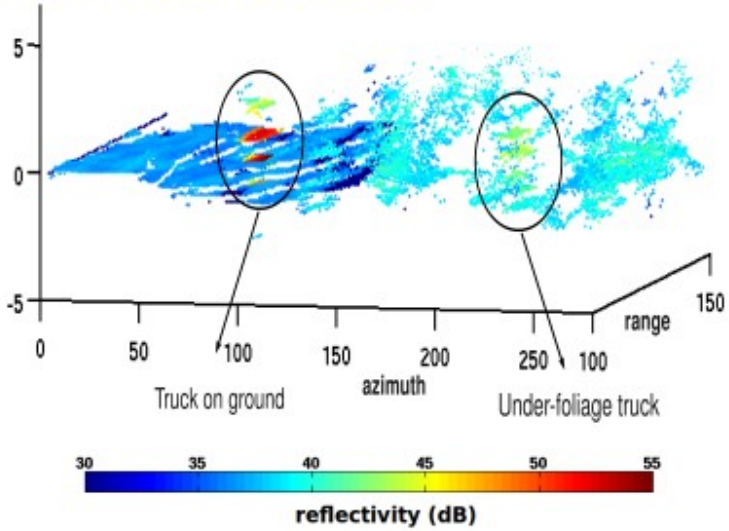

FP-NSF : scattering mechanisms

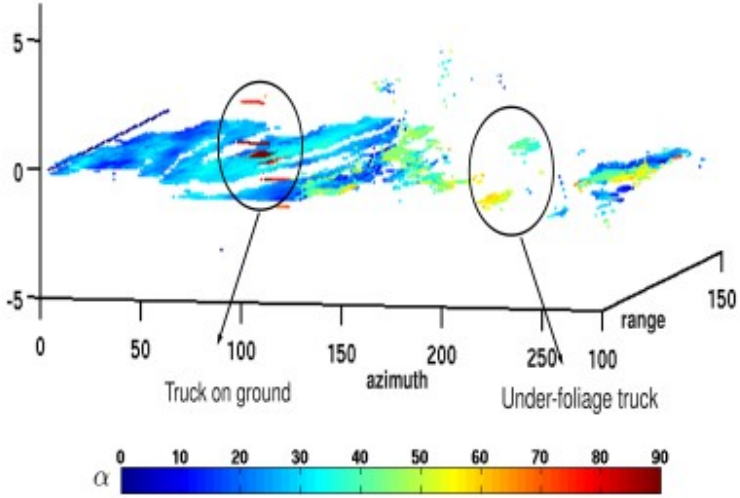

POL-TOMSAR IMAGING OF CONCEALED OBJECTS

Power spectrum of a mixed environment

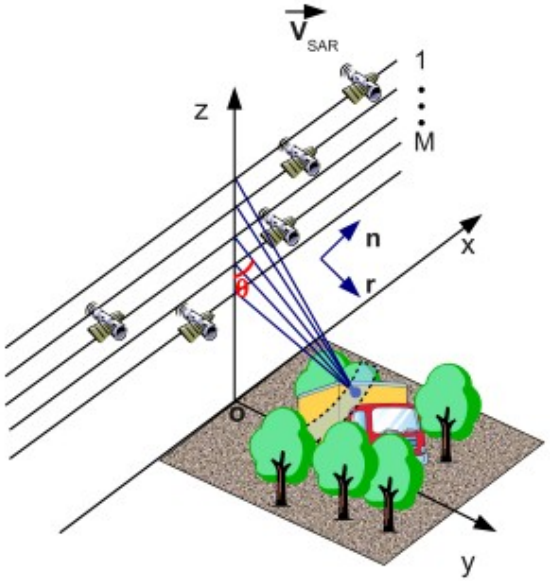

- H-distributed scatterers : Continuous Spectrum
  Forest canopy :

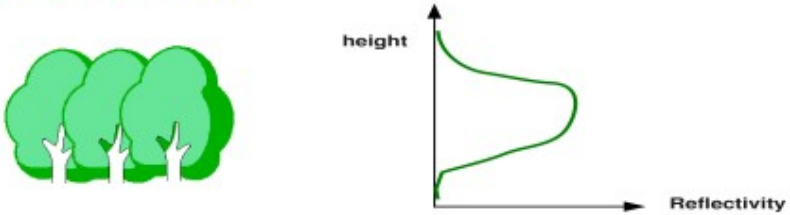

- H-localized scatterers : Discrete Spectrum
  Objects :

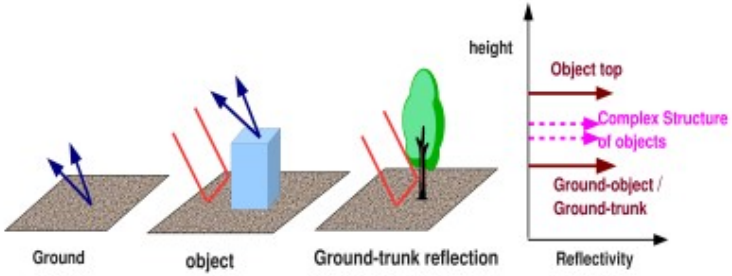

- Underfoliage objects : Mixed-Spectrum

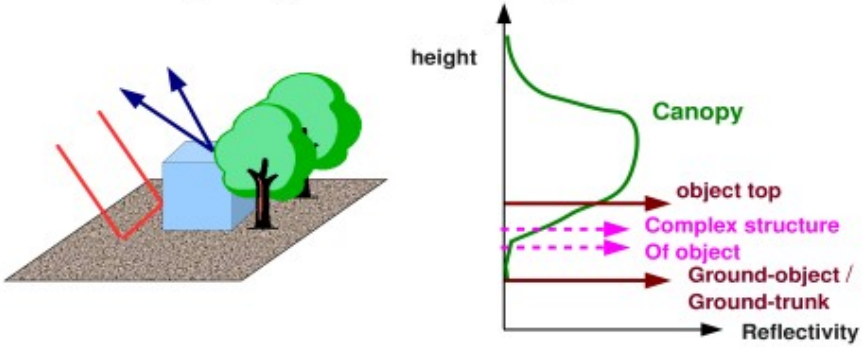

Isolated Scatterer (IS) discrimination

Principle

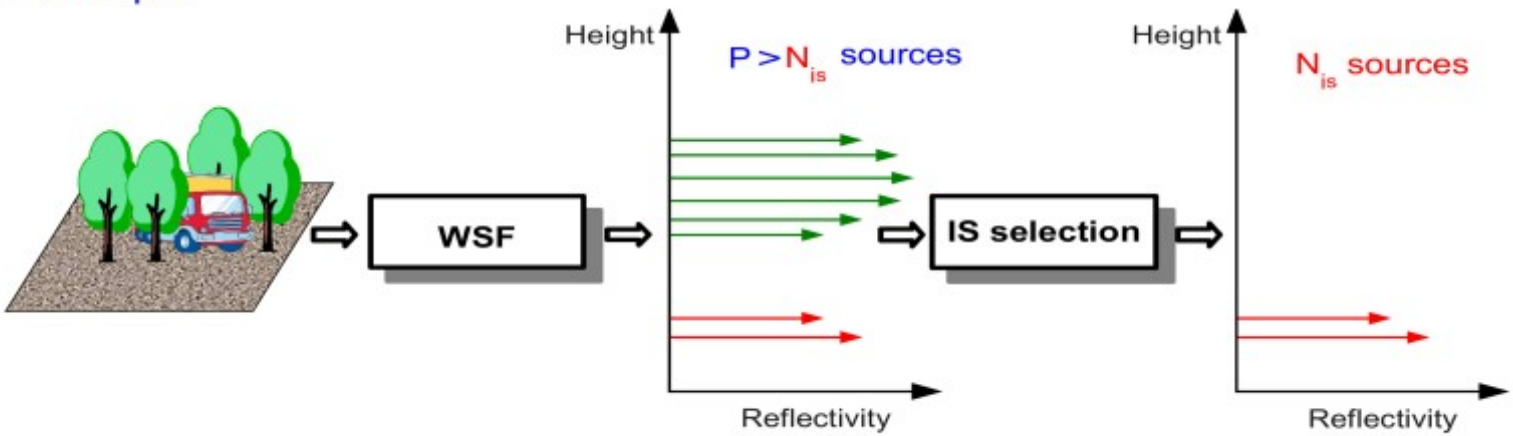

Principle

IS scatterers : stable and coherent scatterers

Diffuse scatterers : unstable scatterers with varying reflectivities

Isolated Scatterer Extraction

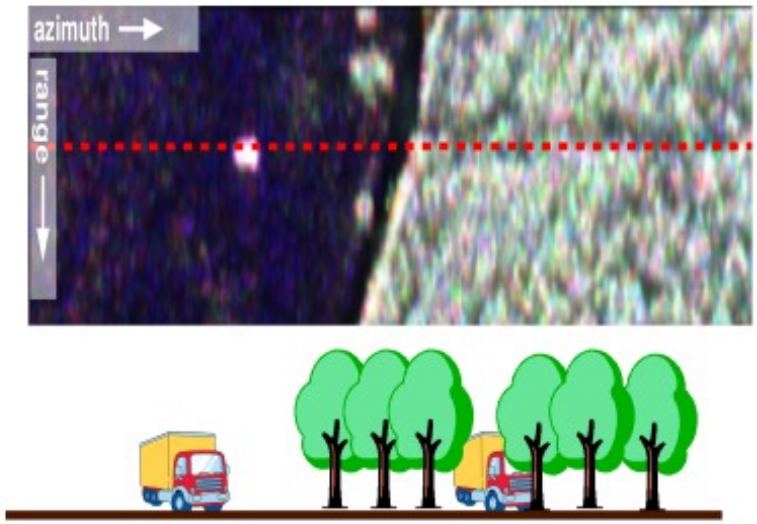

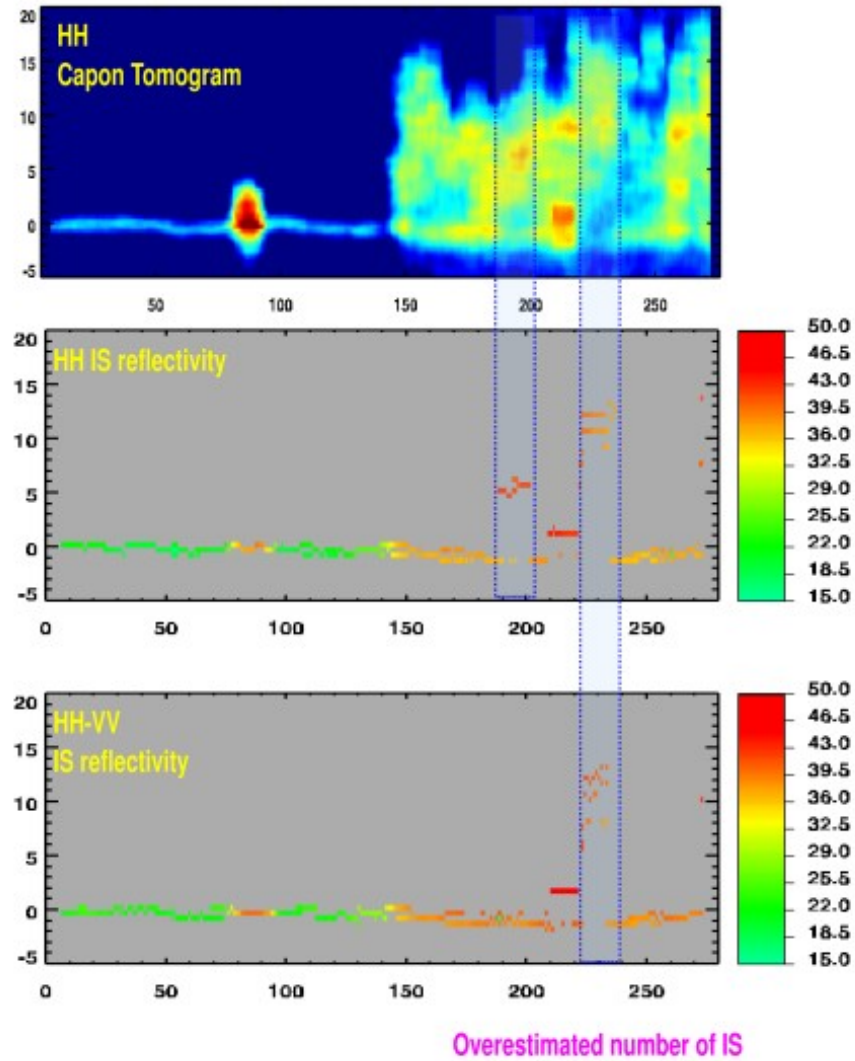

Overestimated IS

- Bare soil, sub-canonpy ground
- Under-foliage truck

POL-TOMSAR IMAGING OF CONCEALED OBJECTS

Single-pol or rank-one polarimetric CAPON

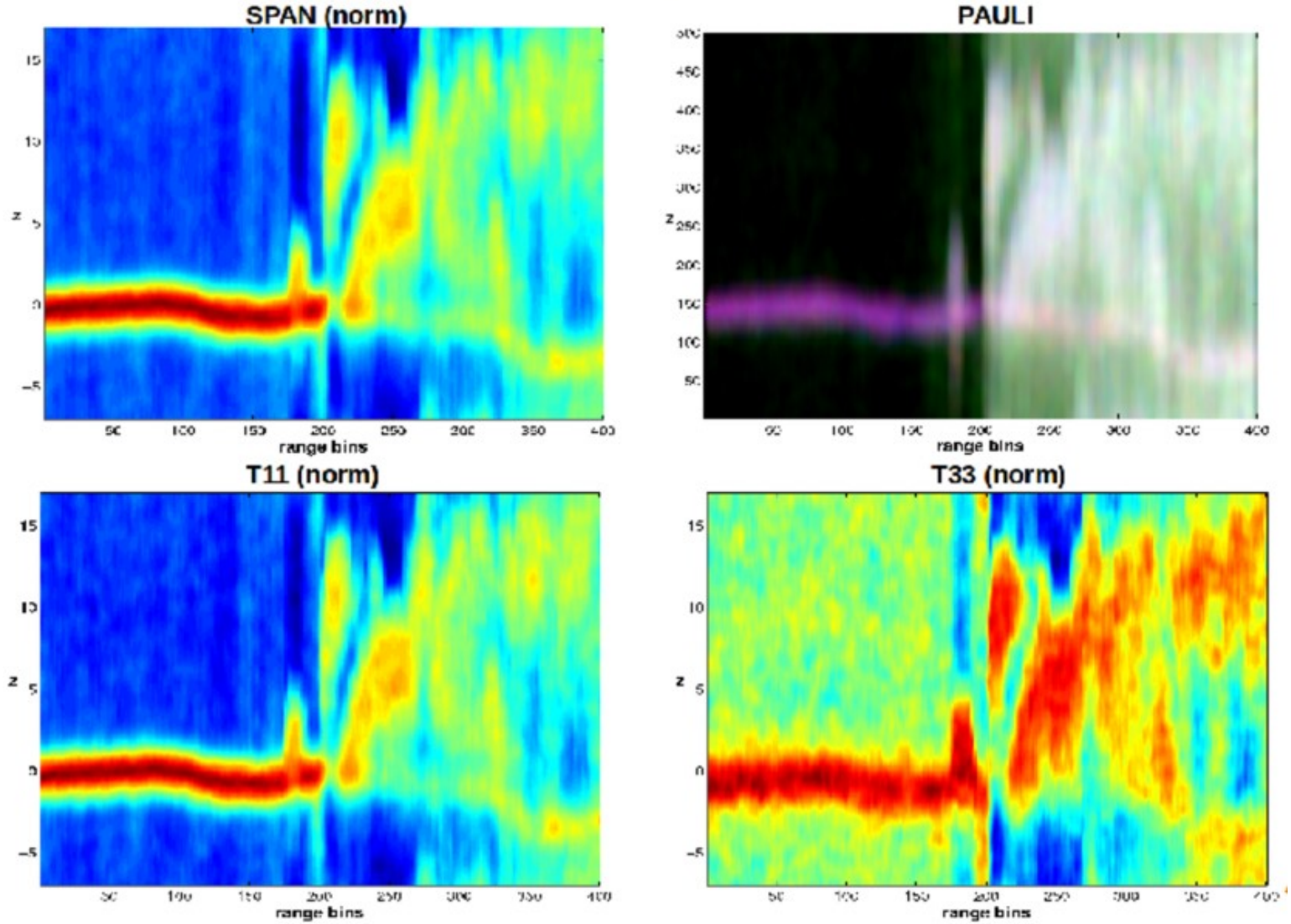

POL-TOMSAR IMAGING OF CONCEALED OBJECTS

Full-Rank Polarimetric CAPON

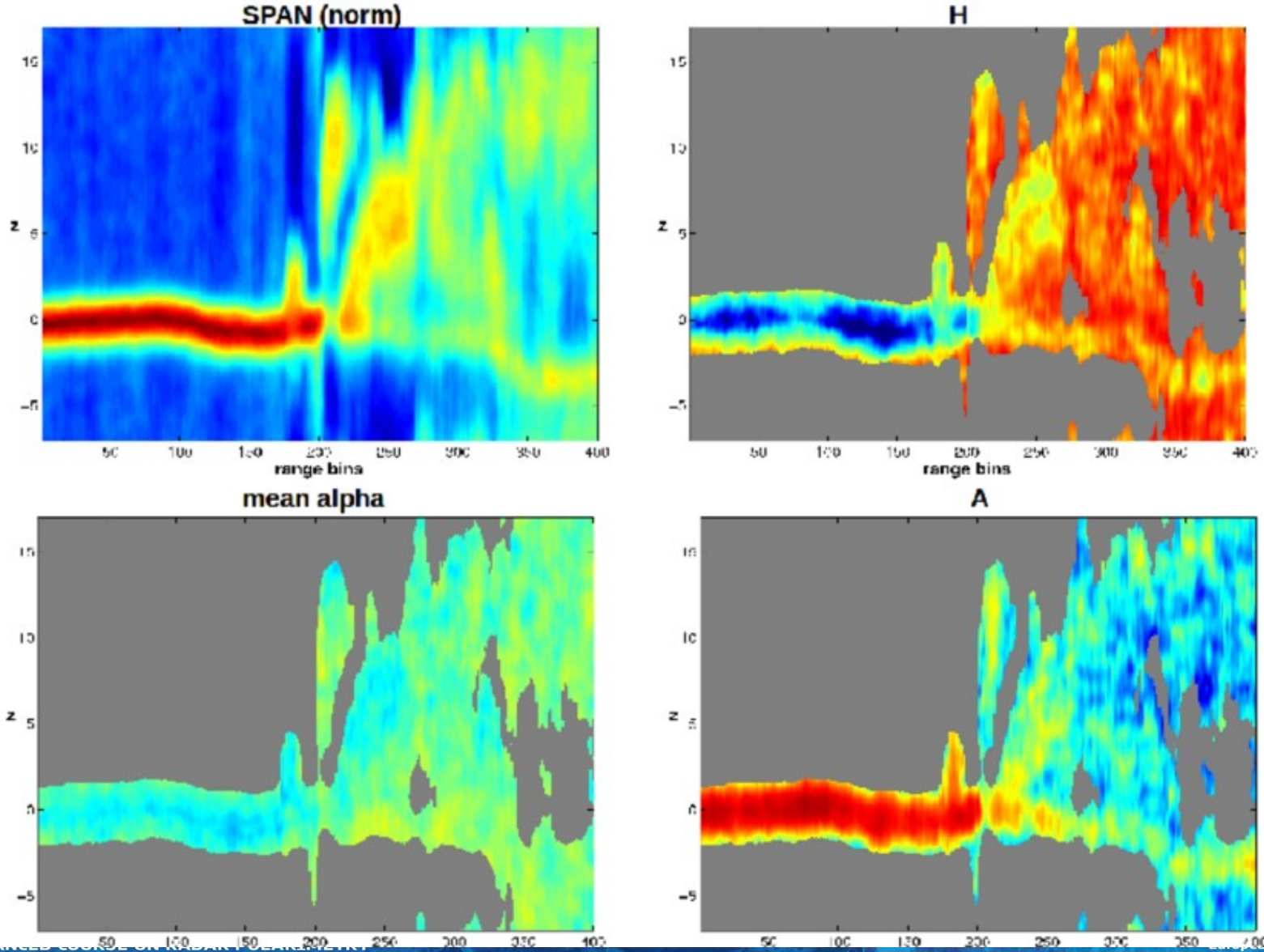

POL-TOMSAR IMAGING OF CONCEALED OBJECTS

Under foliage vehicle detection using FR-P-CAPON and POLSAR techniques

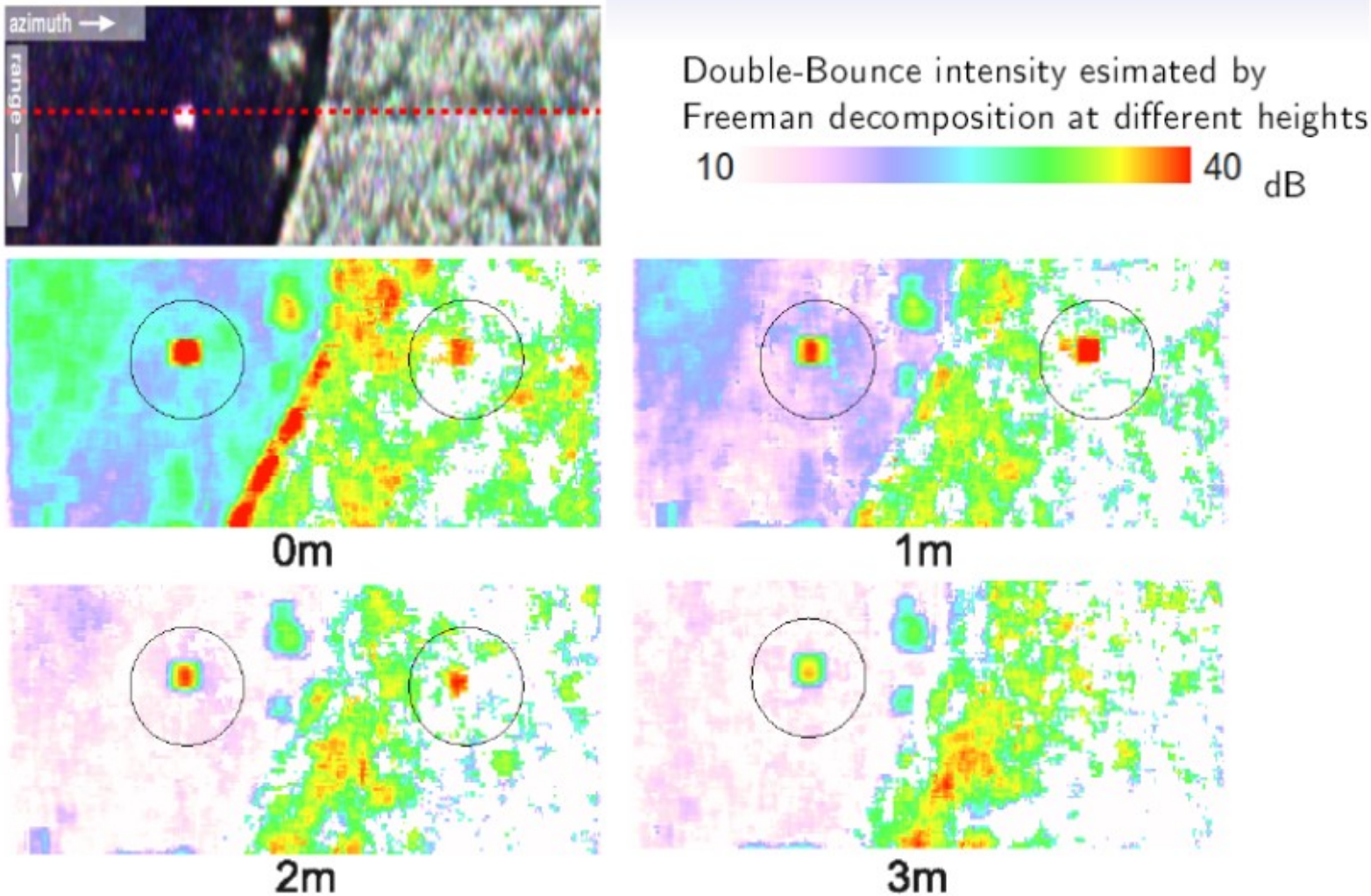

Tropical forest test site and objectives

- TropiSAR Campaign, 2009
- ONERA SETHI
- P-Band
- 6 tracks
- $\delta_{az} = 1.245m$
  $\delta_{rg} = 1m$
- $\delta_z = 12.5m$
- Ground truth
  - LiDAR data
  - Biomass measurements for 16 ROIs

The ECOFOG Sites
- Nouragues
- Paracou
- Arbocel

The Calibration site
- Rochambeau

Other site
- Marais de Kaw

Courtesy ONERA

Objectives

- Tree height,underlying ground topography estimation
- Forest vertical structure characterization
- Biomass monitoring

POL-TOMSAR IMAGING OF A TROPICAL FOREST

Tropical forest test site : Paracou

Optical image

SAR image

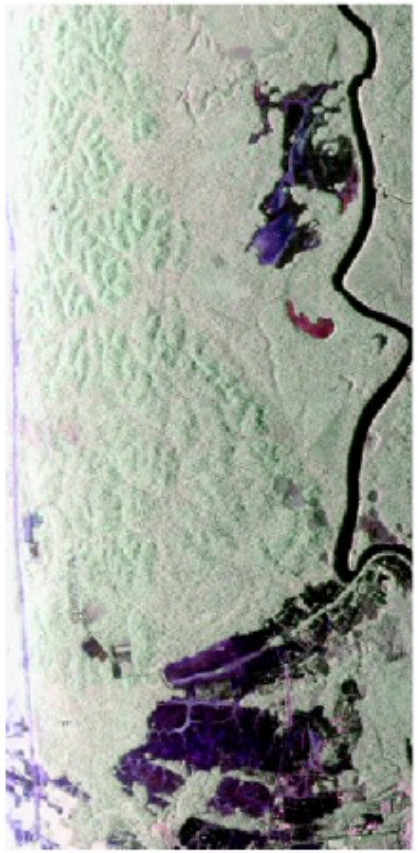

LiDAR z_g

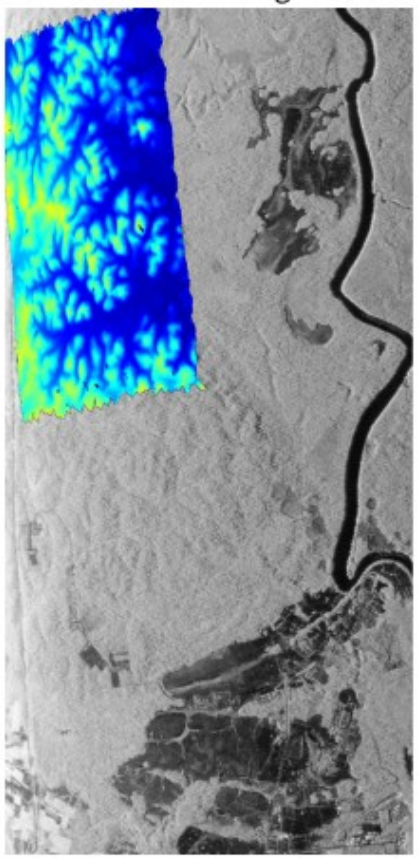

LiDAR z_{top}

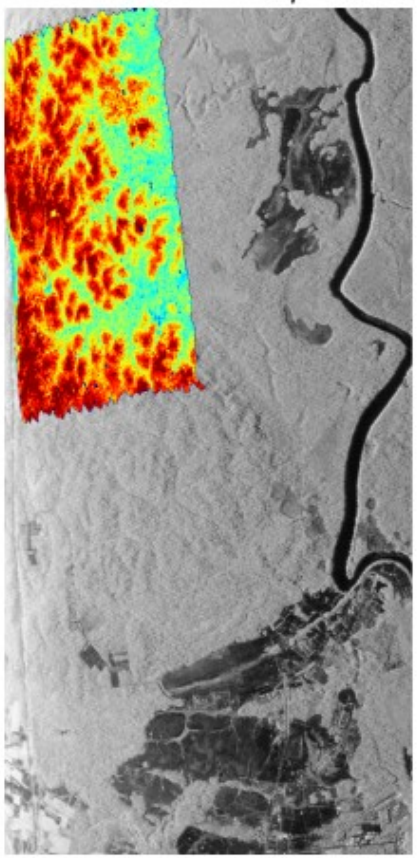

- Tropical forest environments (savannah, undisturbed forests, logged plots...)
- Highly varying ground topography

POL-TOMSAR IMAGING OF A TROPICAL FOREST

Tree height and ground topography estimation

Hybrid spectral approach

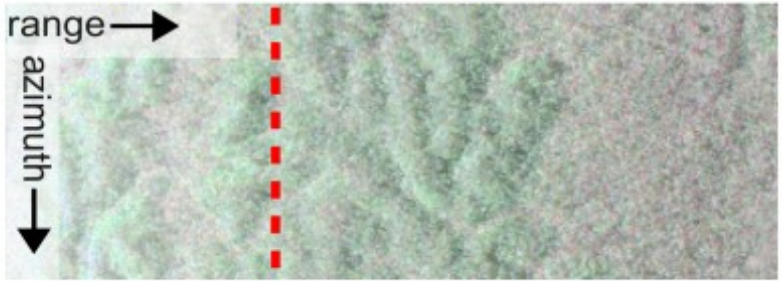

- Estimated profiles match LiDAR
- HH profiles : similar to FP case

LiDAR — TomSAR —

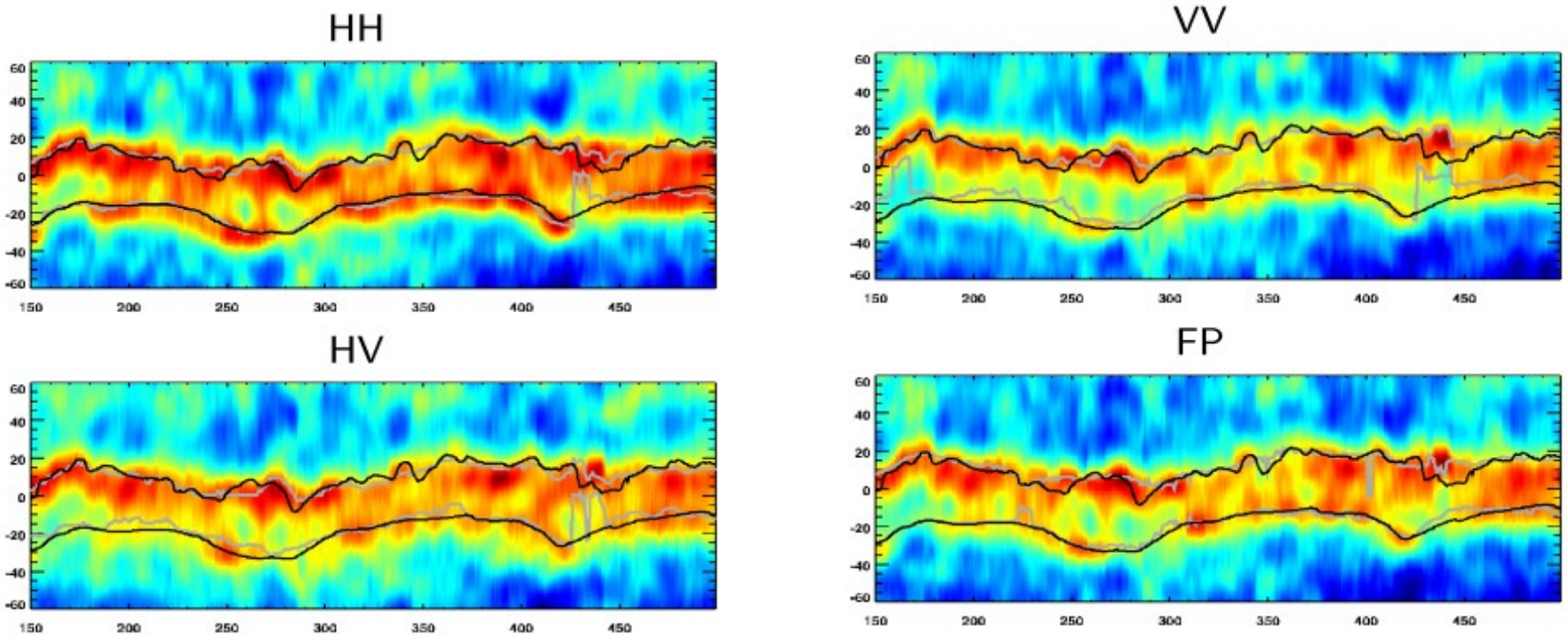

POL-TOMSAR IMAGING OF A TROPICAL FOREST

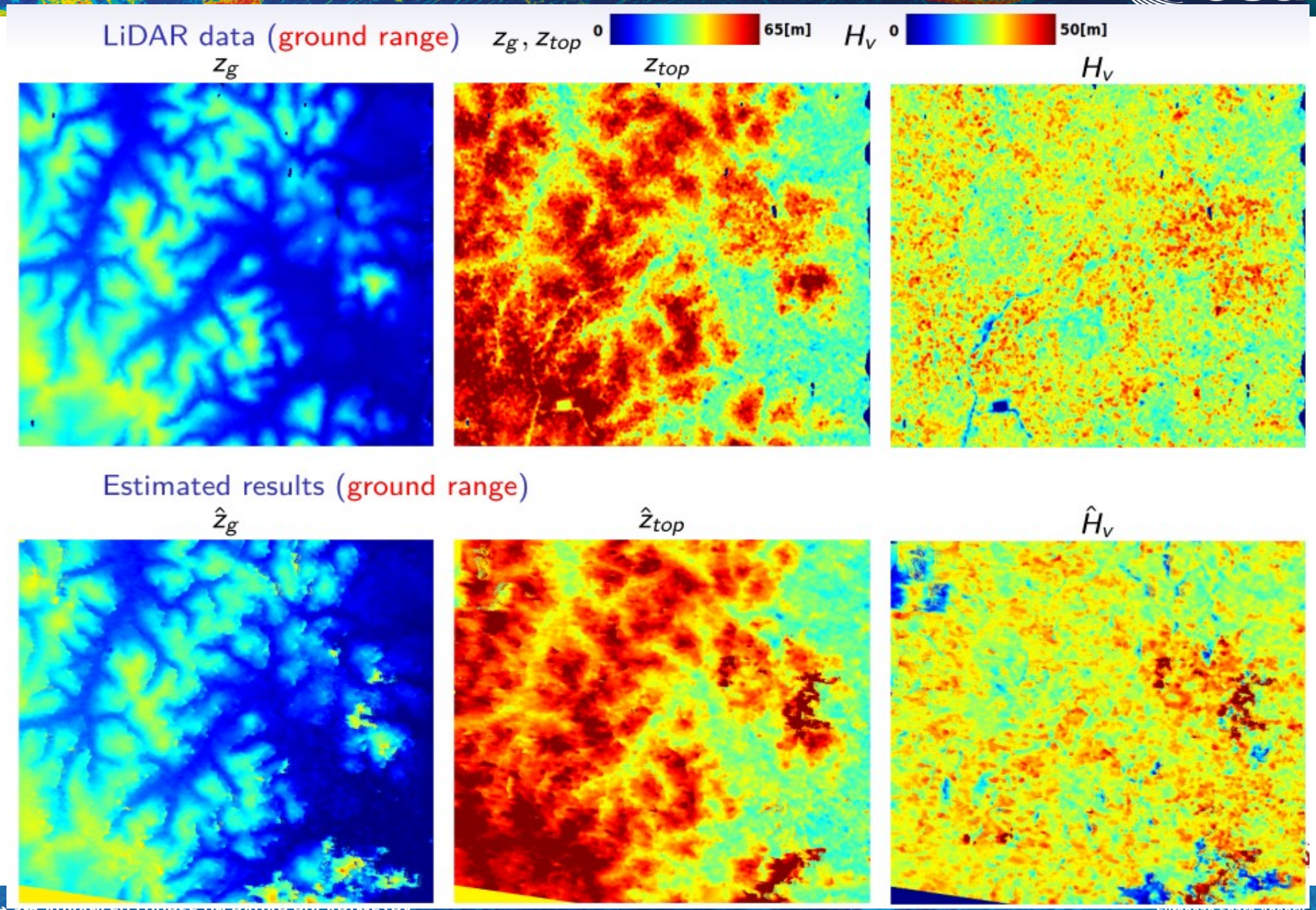

POL-TOMSAR IMAGING OF A TROPICAL FOREST

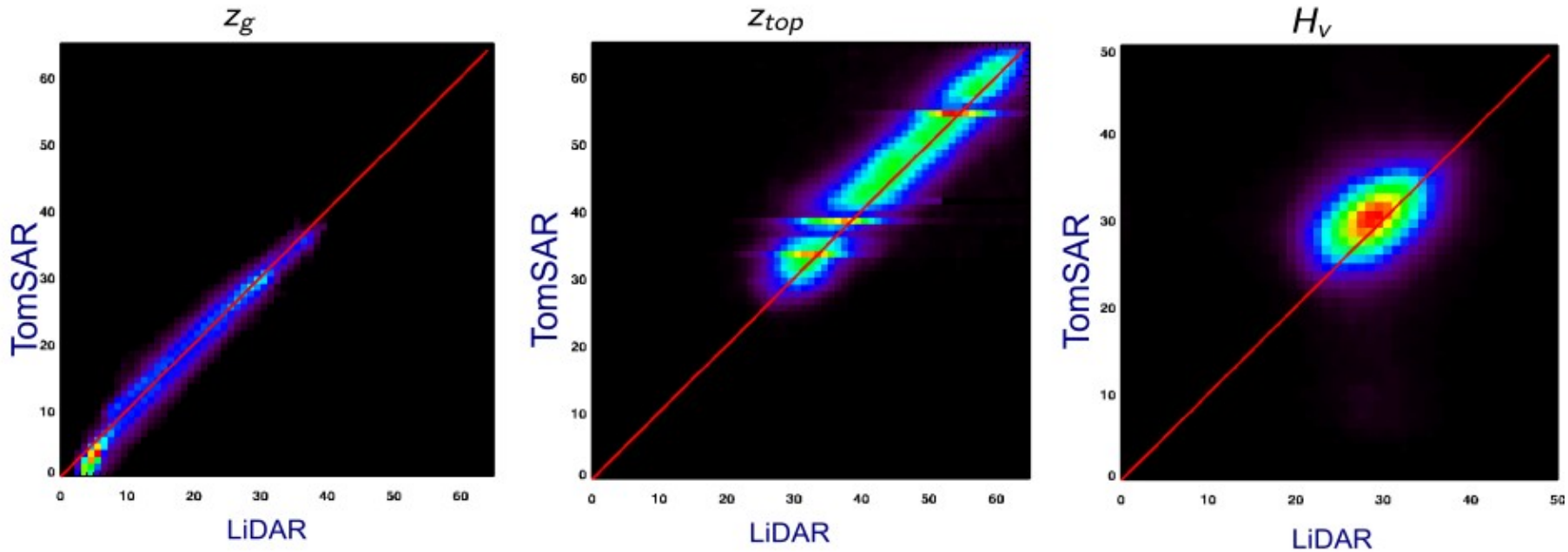

TomSAR-LiDAR [m]	Mean	Std
Δz_g	0.005	4.6
Δz_{top}	1.6	7.4
ΔH_v	0.9	7.7

Full-pol MB-RVOG model

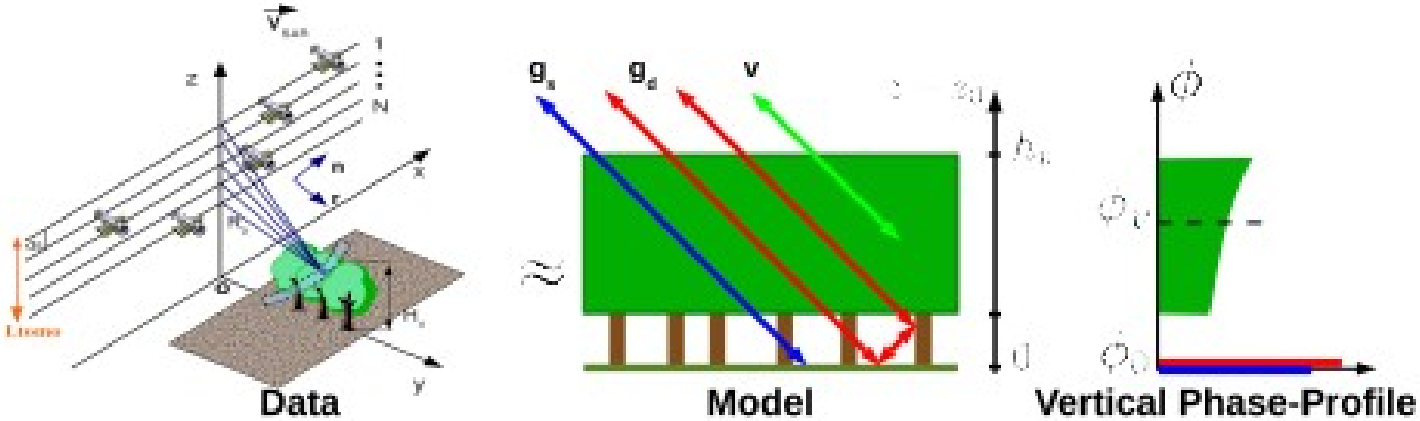

- Point-like scatterer MB-response : $\mathbf{y}(l) = A_c(l) \begin{bmatrix} k_{hh}\mathbf{a}(z) \\ k_{hv}\mathbf{a}(z) \\ k_{vv}\mathbf{a}(z) \end{bmatrix} = A_c(l)\mathbf{k} \otimes \mathbf{a}(z)$
- Uncorrelated P-S processes : $\mathrm{E}(\mathbf{y}_i\mathbf{y}_i^\dagger) = I_i\mathbf{C}_i \otimes \mathbf{R}_i$
- Global MB-POLinSAR response : $\mathbf{y}(l) = \mathbf{y}_g(l) + \mathbf{y}_v(l)$

$$\mathbf{R}_{PS} = \mathbf{C}_g \otimes \mathbf{R}_g + \mathbf{C}_v \otimes \mathbf{R}_v$$

Tebaldini, S. "Algebraic Synthesis of Forest Scenarios From Multibaseline PolInSAR Data", IEEE TGRS 2009
Tebaldini, S. "Single and Multipolarimetric SAR Tomography of Forested Areas: A Parametric Approach" IEEE TGRS 2010

MB-RVOG parameter estimation

SB case

- Coherence line estimation
- GV separation : strong assumptions
  - $|\gamma_g| = 1$, $\text{rank}(\mathbf{C}_g) < 3$
  - $f_v(z)$ known

MB case

- SVD SKP-2 decomposition
- GV separation :
  - several solutions
  - accuracy increases with N_s

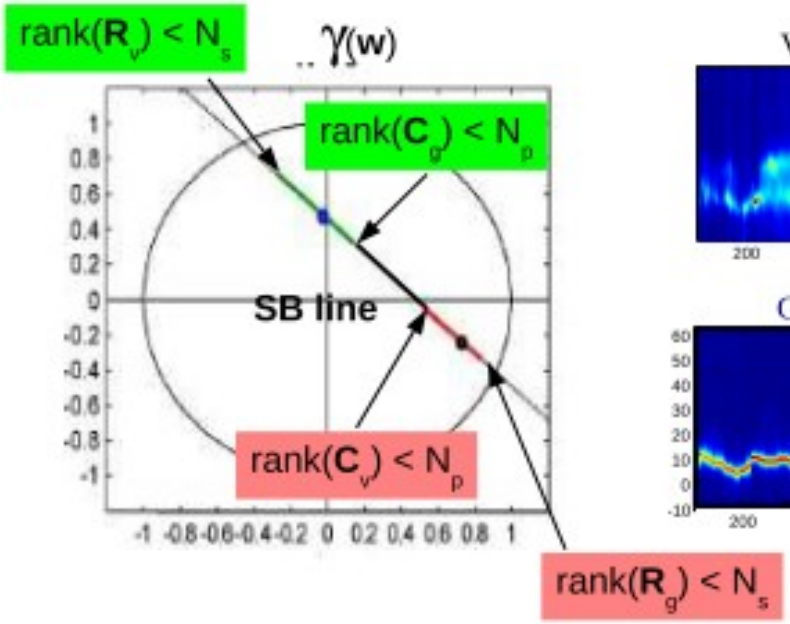

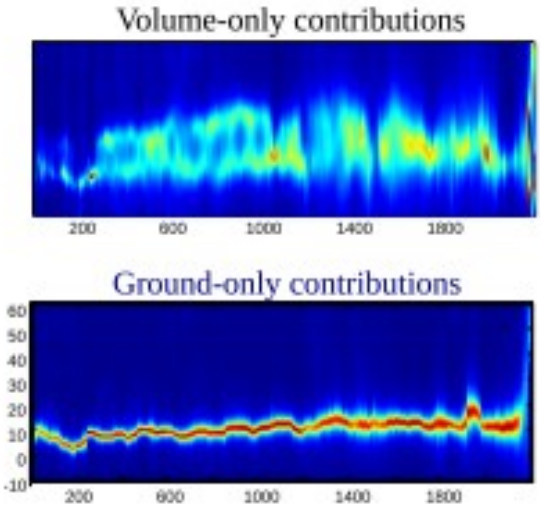

Tebaldini, S. "Algebraic Synthesis of Forest Scenarios From Multibaseline PolInSAR Data", IEEE TGRS 2009
Tebaldini, S. "Single and Multipolarimetric SAR Tomography of Forested Areas: A Parametric Approach" IEEE TGRS 2010

POL-TOMSAR IMAGING OF A TROPICAL FOREST

Interpretation of the different selected solutions

azimuthal cut

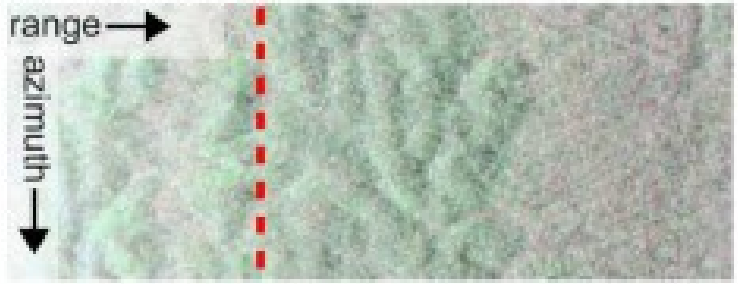

$|HH|^2$ total contribution

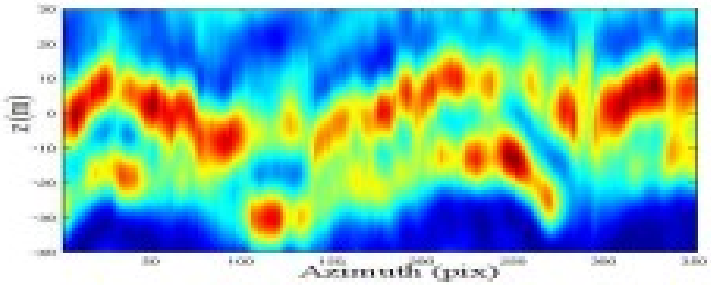

$|HH|^2$ ground with $a = a_{inner}$

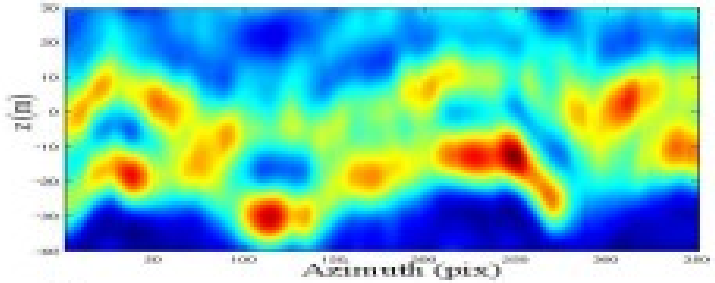

$|HH|^2$ ground with $a = a_{outer}$

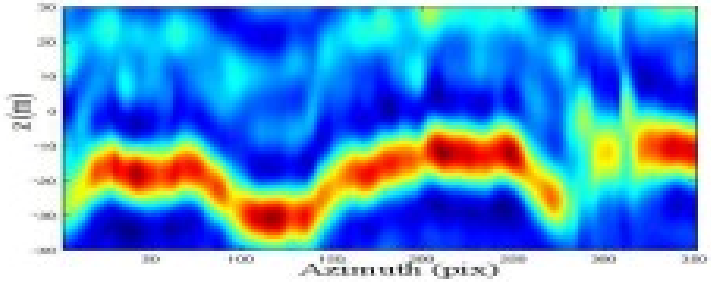

$|HH|^2$ volume with $b = b_{inner}$

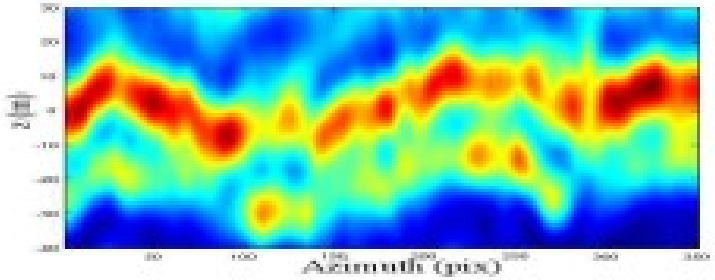

$|HH|^2$ volume with $b = b_{outer}$

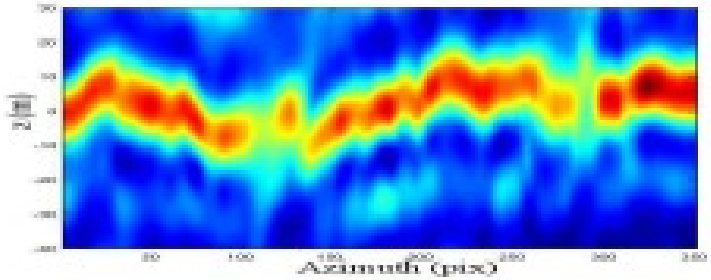

POL-TOMSAR IMAGING OF A TROPICAL FOREST

Full-rank polarimetric CAPON Tomograms : SKP2 matrix

- BF,CAPON : non-parametric approaches
- SP : $\sigma(z)$, FP : $\mathbf{k}_{eq}(z)$, FP-Full rank : $\mathbf{T}(z)$

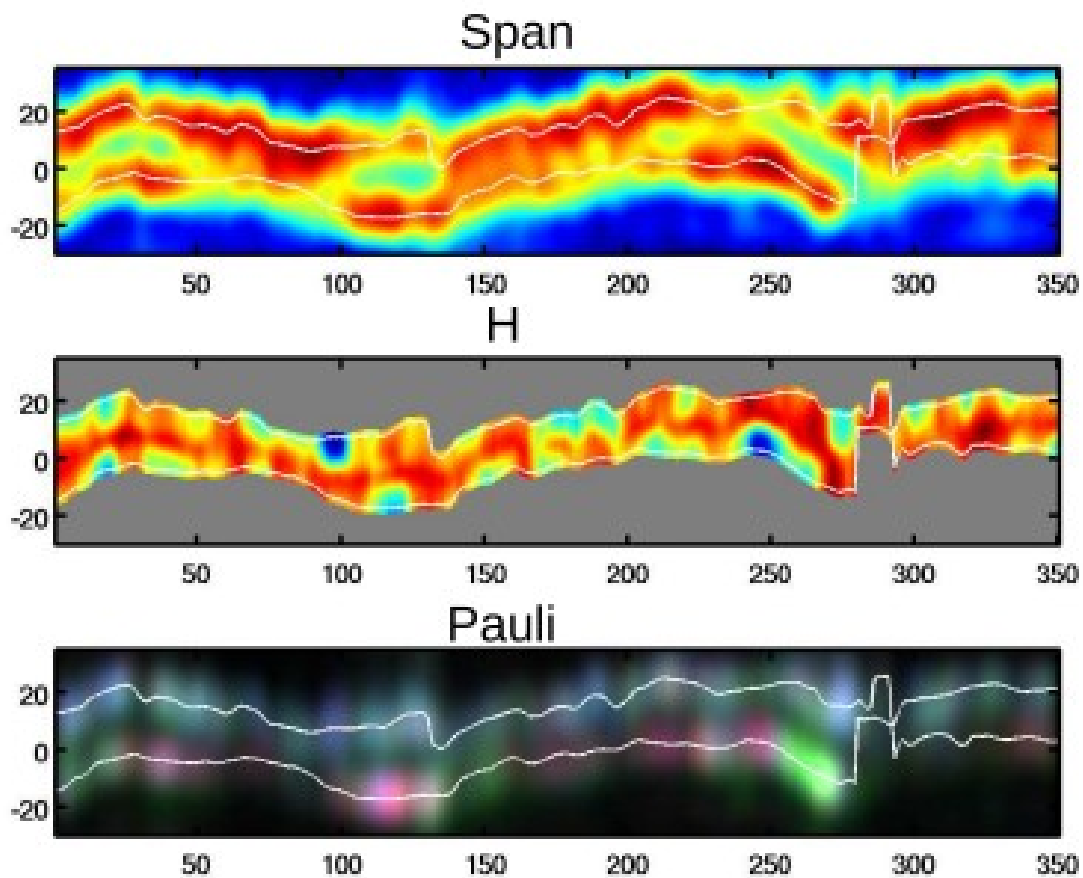

Choosing context adaptive b solutions

$$\mathbf{R_v} = b\mathbf{R_1} + (1-b)\mathbf{R_2} \quad \mathbf{C_g} = \frac{1}{a-b}\left((1-b)\mathbf{C_1} - b\mathbf{C_2}\right)$$

- Terrain polarimetry : $b_g = \arg\min(||\mathbf{C}_g(b) - \mathbf{C}_{CAPON}(z = z_g)||_F^2) \Rightarrow \mathbf{R}_{vol}$
- Canopy structure : $b_{can} = \min b | CAPON(\mathbf{R}_v(b), z = z_g) \rightarrow 0 \Rightarrow \mathbf{R}_{vol}$

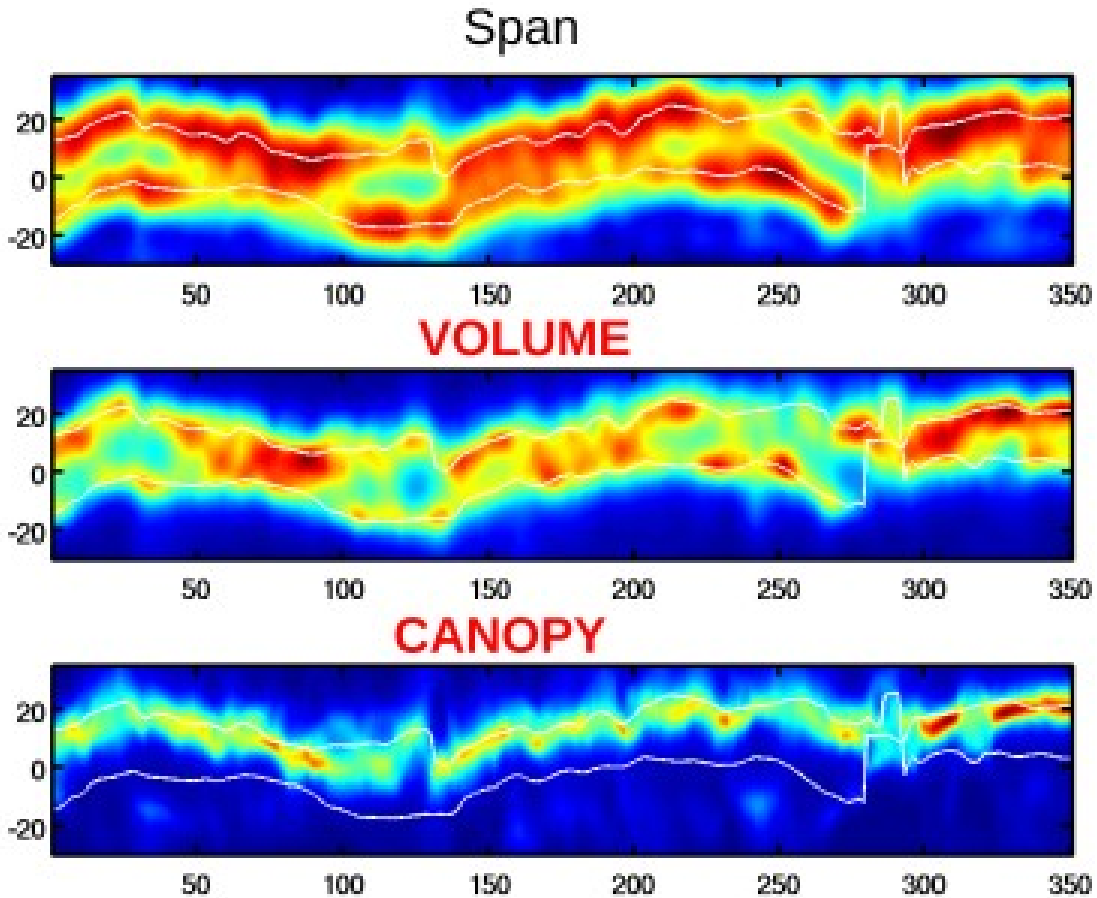

Choosing context adaptive a & b solutions

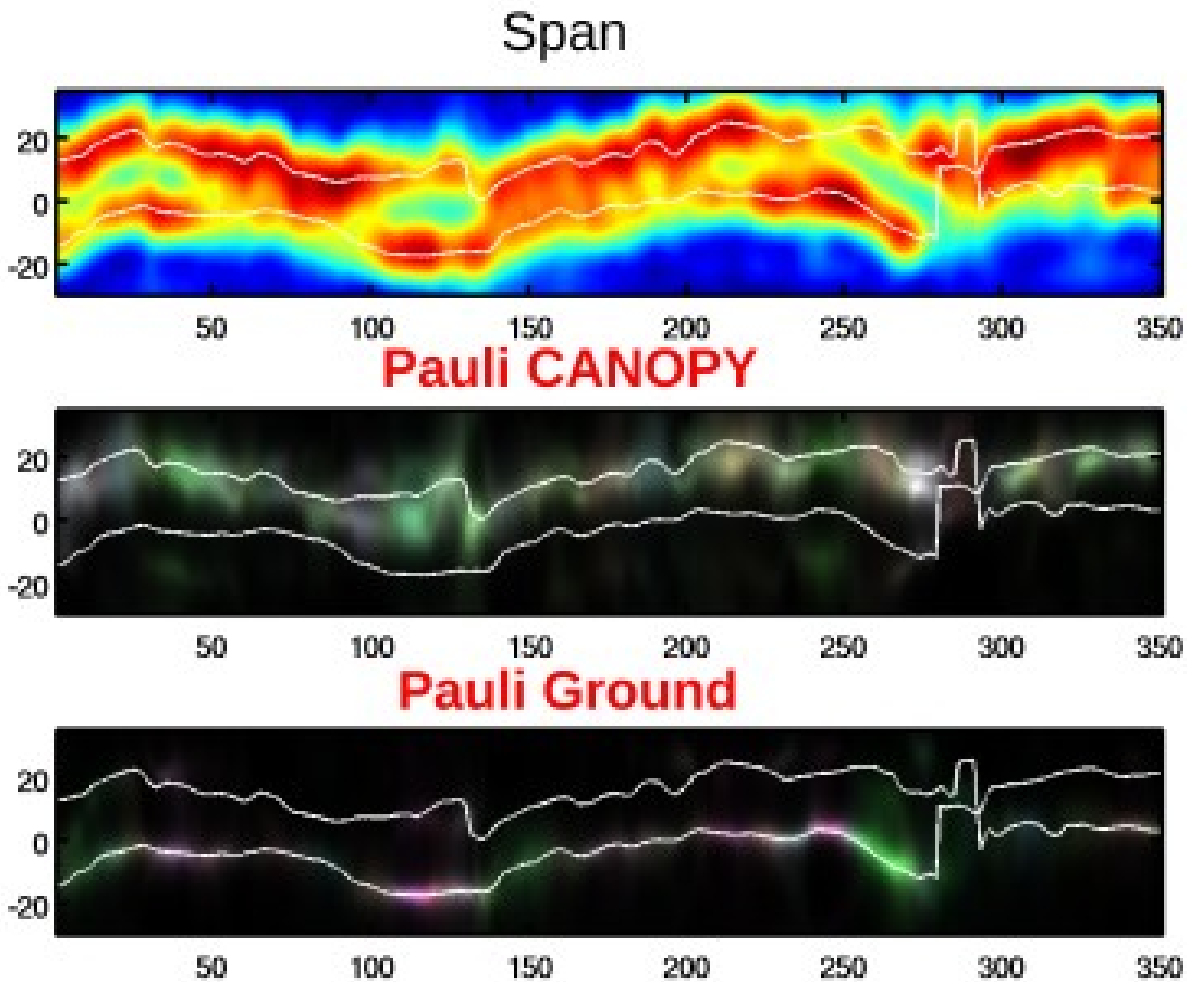

Urban tomography using sparse techniques

Sparse signals

contain a few contributions + artefacts

Objective

characterize a minimal number of sources which describe well the measured signal

Noise filtering

generally performed using SLC data (without averaging)

automatically performed in the stack dimension (source model + sparsity driven technique)

Sparsity-driven technique

Iteratively Reweighted Least-Squares (discards contributions too far from the model)

Urban tomography using sparse techniques

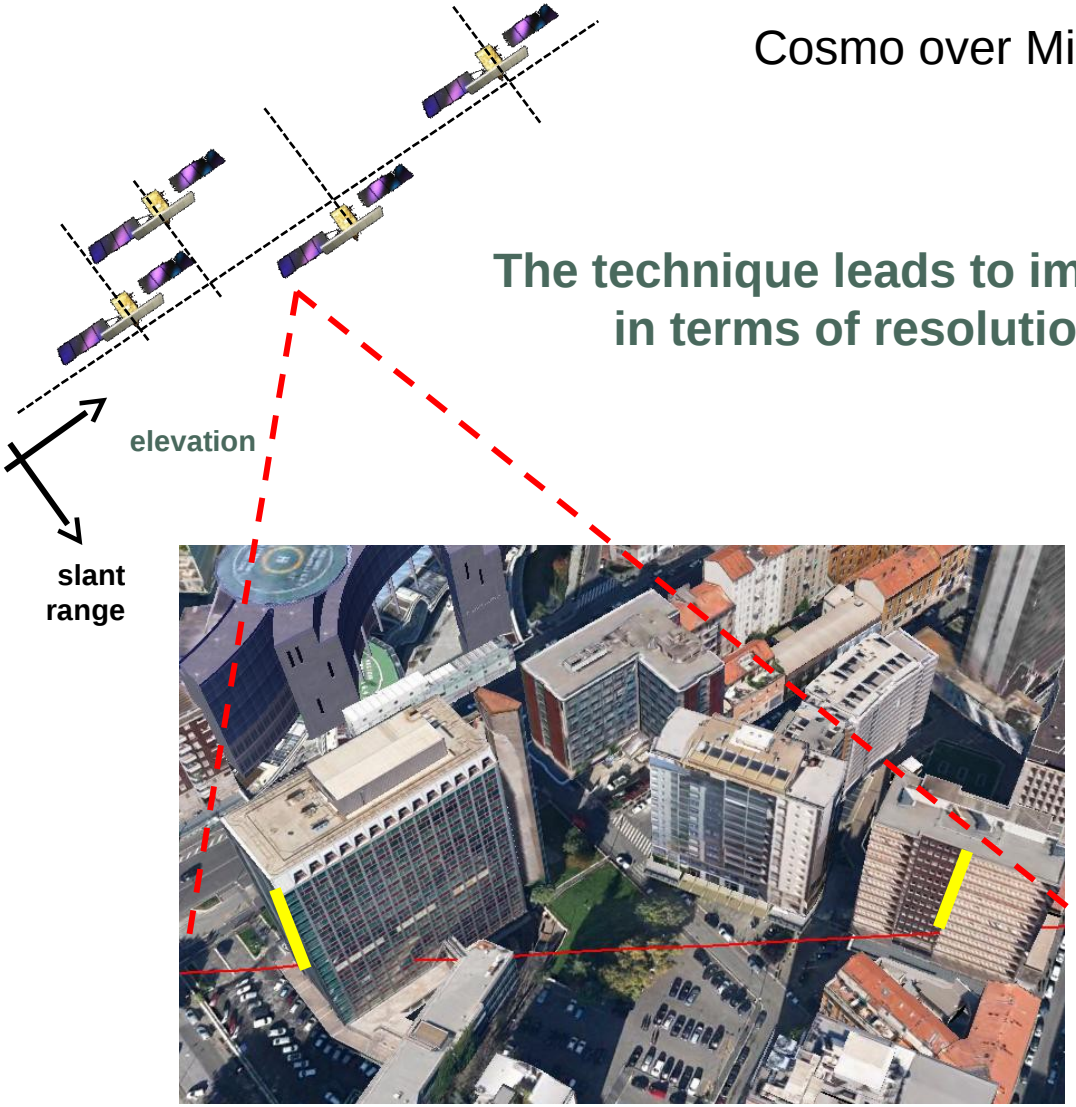

Cosmo over Milan

The technique leads to improvements in terms of resolution and image contrast.

Beamforming

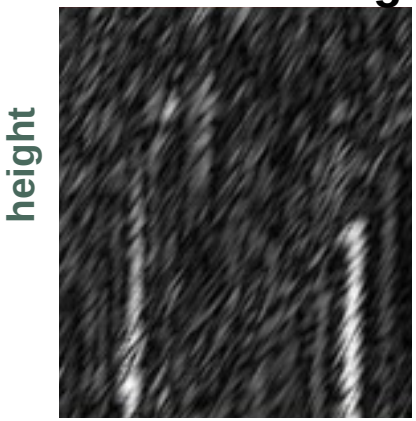

IRLS norm L1

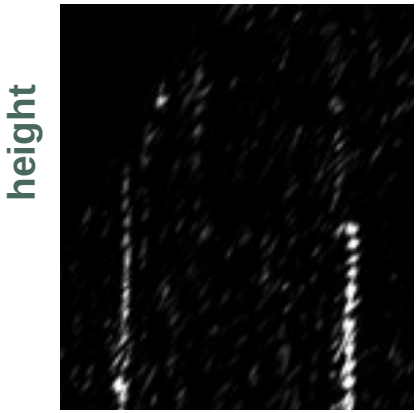

Ground range

Urban tomography using sparse techniques

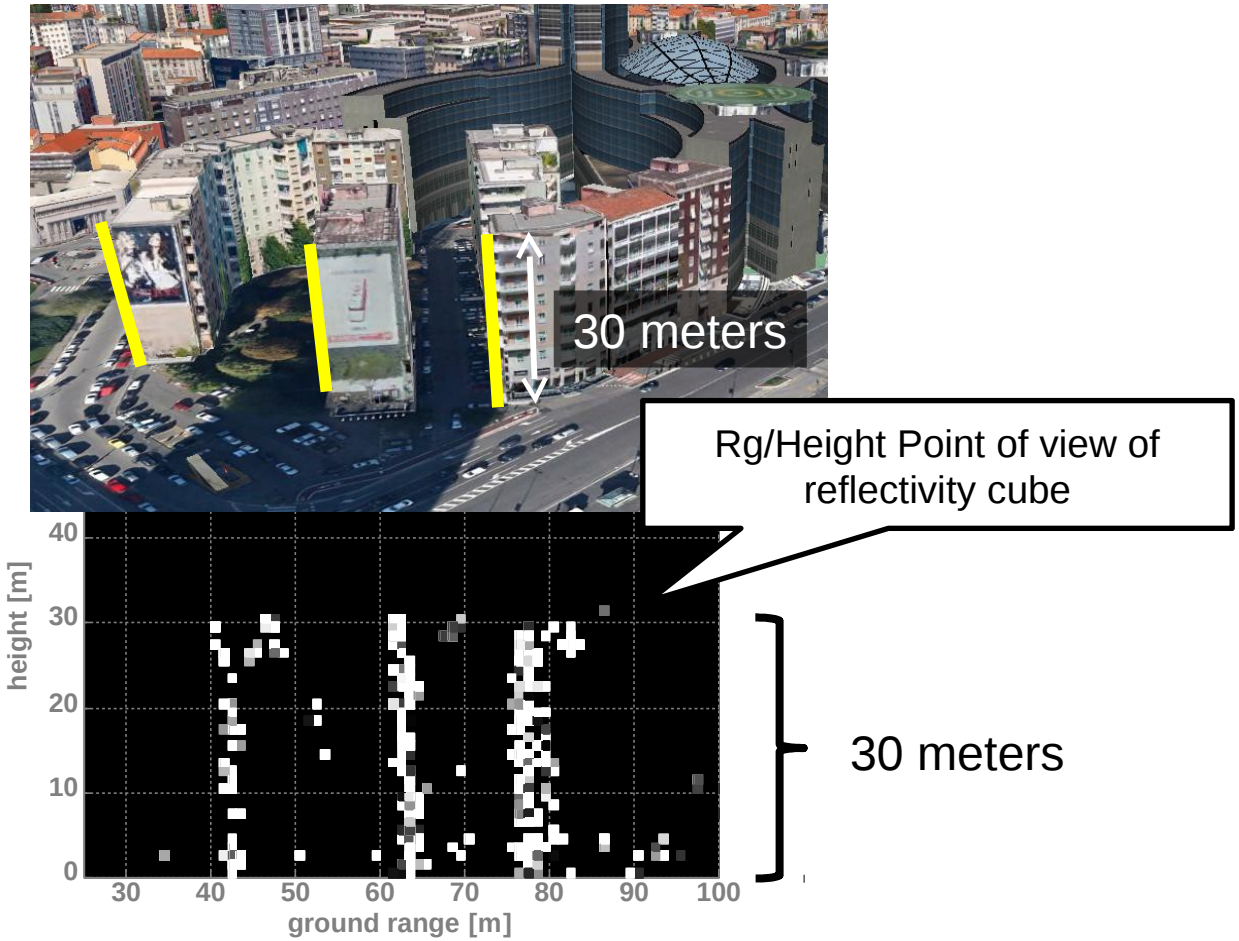

Urban tomography using sparse techniques

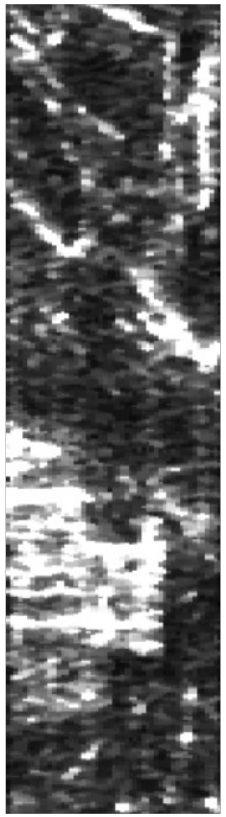

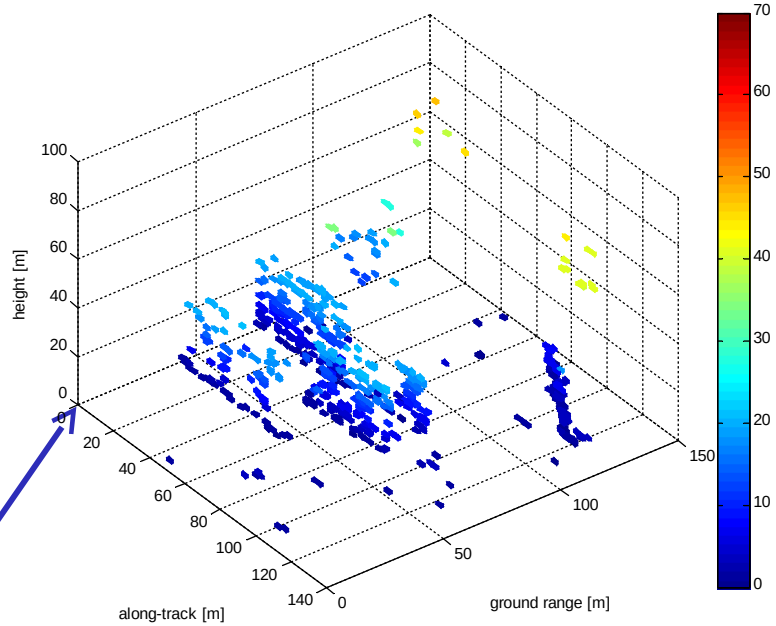

- In order to perform the step from the 2D to 3D a thresholding procedure is necessary.
- The façade structure reconstruction is a typical application of the 3D SAR imaging.

Urban tomography using sparse techniques

- TomoSAR techniques displacing targets in their correct position in the space allow to produce images not affected by layover effect.

Building image from google earth

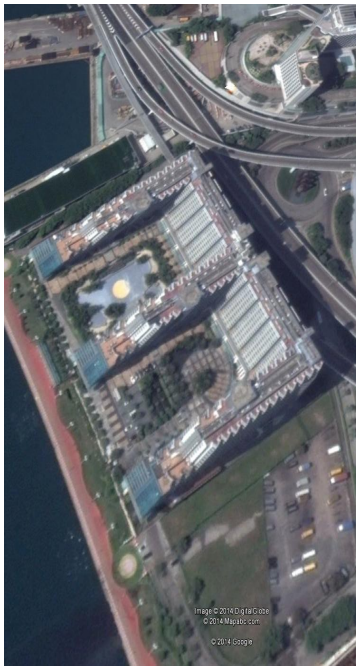

2D SAR

3D SAR
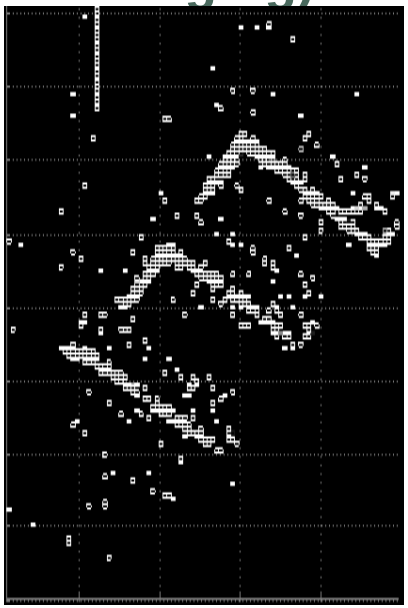
(top view of 3D imaging)